Table 1. Maps relevant to genes for which the expression was affected in the liver of ConA-injected mice followed by ADSC treatment at 3 h.

Maps	*p*-value
Tissue remodeling and wound repair	0.000001438
Inflammatory response	0.000003973
Mitogenic signaling	0.0001056
Vascular development (angiogenesis)	0.0002926
DNA damage response	0.0004529
Apoptosis	0.0008909
Cystic fibrosis disease	0.001402
Myogenesis regulation	0.001571
Cell differentiation	0.002173
Immune system response	0.003304

In conclusion, the therapeutic anti-inflammatory efficacy of ADSCs relied on suppression of myeloid-lineage and $CD4^+$ T cells in the ConA-induced C57BL/6 murine hepatitis model. The application of ADSC therapy to various inflammatory liver diseases can be further developed by studies of their immunomodulatory effects.

Materials and methods

Murine acute hepatitis induced by ConA injection and treatment with ADSCs

C57BL/6J female mice (10–12 weeks old, Charles River Laboratories Japan Inc., Yokohama, Japan) were injected i.v. with 300 μg of ConA (Sigma-Aldrich, St. Louis, MO, USA) dissolved in PBS. For $CD4^+$ T-cell or $CD8^+$ T-cell depletion, 200 μg of purified anti-CD4 antibody from the culture supernatant of GK1.5 cells (ATCC, Manassas, VA, USA), or purified anti-CD8 antibody from the culture supernatant of 2.43 cells (ATCC), was injected i.p. for two consecutive days before ConA injection. For depletion of monocyte-macrophage lineage cells, 2 mg of clodronate (Sigma-Aldrich), which was encapsulated in liposomes using the COATSOME-EL-01-N liposome formulation kit (Nihonyushi, Tokyo, Japan) [27], was injected via the tail vein 2 days before ConA injection. For the prevention or treatment experiment, 1×10^5 ADSCs were administered i.v. immediately or 3 h after ConA injection. In some cohorts, blood was obtained under anesthesia, and liver and lung tissues were collected after euthanizing mice at 6, 12, and 24 h after ConA injection. A portion of the liver tissue was homogenized and the enriched fraction of inflammatory cells was obtained by gradient centrifugation using Ficoll–Hypaque (Sigma-Aldrich). Our institutional review board approved the care and use of laboratory animals in all experiments.

Isolation and culture of ADSCs and primary hepatocytes

Inguinal adipose tissues were obtained from C57BL/6J male mice (10–12 weeks old, Charles River Laboratories Japan Inc.) or GFP-transgenic mice (male, 10–12 weeks old, gift from Prof. Okabe, Osaka University, Japan). Tissues were digested with 0.075% collagenase type I (Wako Pure Chemical Industries Ltd., Osaka, Japan), washed with PBS, and then transferred to a culture dish with DMEM/F-12 1:1 medium (Life Technologies–Invitrogen, Carlsbad, CA, USA) supplemented with 10% heat-inactivated FBS and 1% antibiotic–antimycotic solution (Life Technologies). Cells were maintained and expanded by eight to ten passages before use.

To obtain primary hepatocytes, C57BL/6J male mice (10–12 weeks old) were anesthetized by i.p. injection of pentobarbital (50 mg/kg; Kyoritsu Seiyaku, Tokyo, Japan) and injected with 10 mL of 0.75% type I collagenase solution via the portal vein. Liver tissues were minced to dissociate cells, filtered through a 100 μm mesh, and cultured in 10-cm culture dishes for 16 h until use.

Pluripotency of ADSCs

The pluripotency of ADSCs was examined using a mouse mesenchymal stem cell functional kit® (R&D Systems, Minneapolis, MN, USA), and immunohistochemical staining of cells that had differentiated into osteocytes, chondrocytes, and adipocytes was performed using anti-mouse ostepontin, anti-mouse collagen II, and anti-mouse FABP4 antibodies, respectively, in accordance with the manufacturer's instruction. Adipocyte differentiation was also assessed by staining using an aliquot of Oil Red O (WAKO).

Co-culture of ConA-stimulated hepatic inflammatory cells with ADSCs

Hepatic inflammatory cells were isolated from C57BL/6J female mice (10 weeks old) that had been injected i.v. with 300 μg of ConA 3 h before ($n = 4$). $CD4^+$ T cells and $CD11b^+$ cells were separated from the collected hepatic inflammatory cells using anti-CD4 and anti-CD11b magnetic beads (Miltenyi Biotec, Bergisch Gladbach, Germany). Then, 20 000 ADSCs were co-cultured with 4×10^5 of the isolated $CD4^+$ T cells or $CD11b^+$ cells in a 24-well plate (BD Falcon, San Jose, CA, USA) for 2 h ($n = 3$). After co-culture, floating cells were harvested, and RNA harvested using the MicroRNA isolation kit (Stratagene, La Jolla, CA, USA) for real-time PCR analysis to measure cytokine/chemokine gene expression.

Measurement of serum ALT and LDH activity

Blood was collected from the postorbital venous plexus and serum was separated from clotted blood after coagulation. The serum activity of ALT, and LDH was measured using L-type WAKO GPT J2, and LDH-J kits (Wako Pure Chemical Industries Ltd.), respectively, using autoanalytical equipment (Hitach7180, Hitachi Ltd., Tokyo, Japan), according to the manufacturer's protocol.

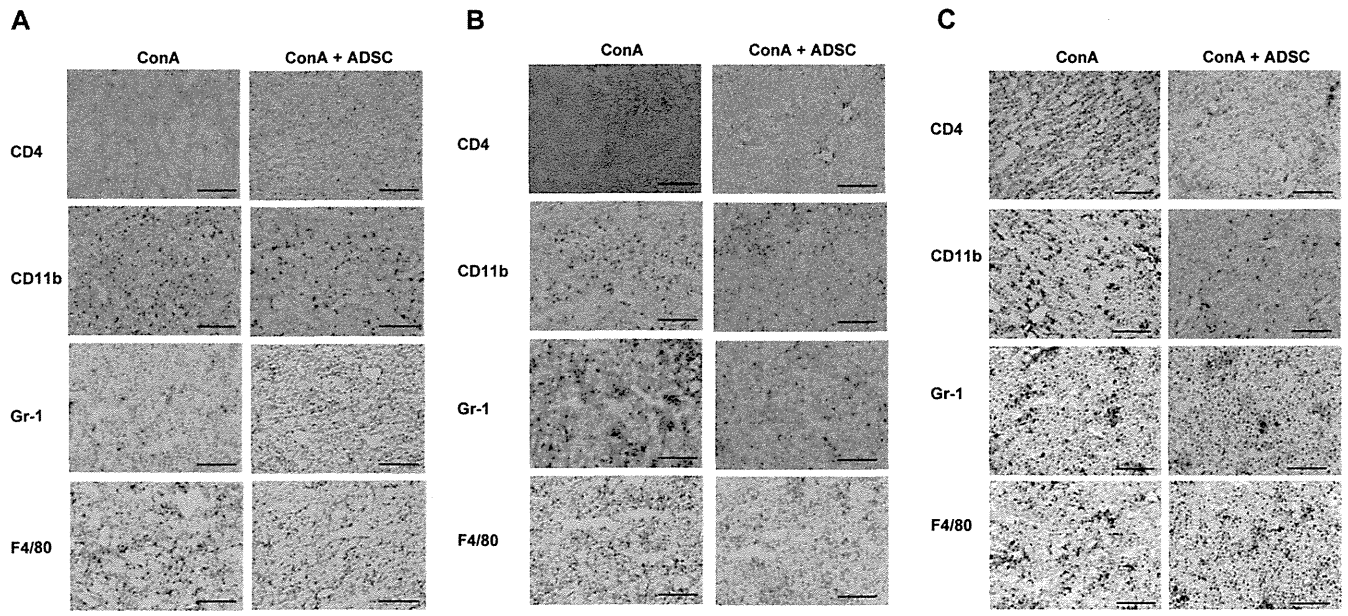

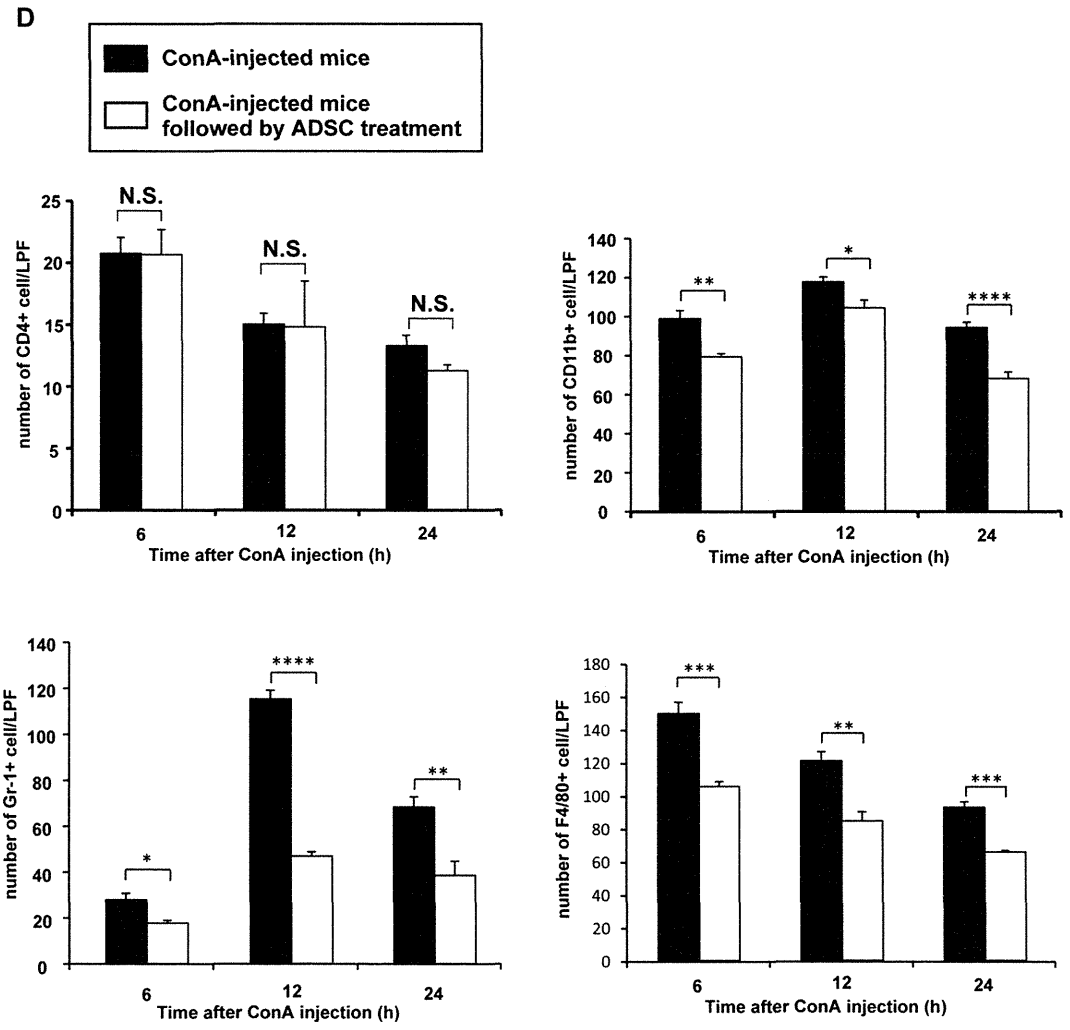

Measurement of serum cytokine/chemokine concentrations

Sera were obtained from ADSC-treated mice immediately or 3 h after ConA injection ($n = 3$ and $n = 4$, respectively), and from ConA-injected mice not treated with ADSCs ($n = 3$ and $n = 6$, respectively) at 6 h. Serum concentrations of cytokines and chemokines were measured using a Multiplex Bead Immunoassays kit, Mouse Cytokine 20-Plex Panel (Invitrogen, Carlsbad, CA, USA), following the manufacturer's protocol. The kit covers FGF-basic, GM-CSF, IFN-γ, IL-1α, IL-1β, IL-2, IL-4, IL-5, IL-6, IL-10, IL-12 (p40/p70), IL-13, IL-17, IP-10(CXCL10), KC, MCP-1, MIG(CXCL9), MIP-1α, TNF-α, and VEGF.

Histological and immunohistochemical analyses of liver and lung tissues

Harvested liver and lung tissues were fixed in 10% formaldehyde, embedded in paraffin, sectioned at 4 μm, and stained with H&E. For immunohistochemical analysis, the liver tissues were embedded in OCT compound (Sakura Finetek, Torrance, CA, USA), snap-frozen in liquid nitrogen, cryostat-sectioned, and fixed with methanol/acetone (1:1). The paraffin-embedded tissues were also sliced into 4 μm sections, mounted on microscope slides, and deparaffinized, followed by epitope retrieval using proteinase K (Dako, Glostrup, Denmark). The slides were incubated with peroxidase blocking reagent (Dako) for 15 min at room temperature to inhibit endogenous peroxidase activity, followed by incubation with protein blocking reagent (Dako) to avoid nonspecific protein reactions. The slides were incubated with primary antibodies (anti-mouse CD4, CD11b, Gr-1, F4/80) (BD Pharmingen, San Diego, CA, USA) and anti-GFP (MBL, Nagoya, Japan) diluted with PBS containing 1% BSA overnight at 4°C. After washing in PBS, the slides were then incubated with secondary antibodies (anti-rat, anti-rabbit; Nichirei, Japan) for 30 min at room temperature. The immune complexes were visualized using EnVision kits /HRP (DAB; Dako) followed by counterstaining with hematoxylin. The numbers of positive cells in each section were counted in four randomly selected fields at 100× magnification under a microscope.

RNA isolation and gene expression analysis by DNA microarray

Total RNA was obtained from the tissues or hepatic inflammatory cells in RNAlater (Ambion) using RNA isolation kit (Sigma-Aldrich) in accordance with the supplied protocol with slight modifications. Isolated RNA was amplified and labeled with the Cy3 using the Quick Amp labeling kit (Agilent Technologies, Santa Clara, CA, USA) in accordance with the manufacturer's protocol. cRNA of 1.65 μg was hybridized onto a Whole Mouse Genome 4 × 44K Array (Agilent Technologies) and scanned using a DNA Microarray Scanner (model G2505B, Agilent Technologies).

Gene expression data were analyzed using the GeneSpring analysis software (Agilent Technologies). Each measurement was divided by the 75th percentile of all measurements in that sample at per chip normalization. Hierarchical clustering and principal component analysis of gene expression was performed. Welch's *t*-test, with Benjamini and Hochberg's false discovery rate, was used to identify genes that were differentially expressed in the groups of interest. Analysis of biological processes was performed using the MetaCore software suite (GeneGo, Carlsbad, CA, USA). BRB array tools (http://linus.nci.nih.gov/BRB-ArrayTools.html) were also used for unsupervised or one-way clustering analyses. Microarray data were deposited in the NBCI Gene Expression Omnibus (GSE ID: GSE41465).

Flow cytometry

Cultured ADSCs were incubated in PBS supplemented with 2% BSA (Sigma-Aldrich) containing antibodies labeled with FITC or PE anti-mouse CD44 or CD90 (Beckman Coulter, Brea, CA, USA), and CD105 (Miltenyi Biotec) antibodies. Hepatic inflammatory cells isolated from mice were incubated with a mixture of FITC-labeled anti-mouse CD204 (AbD Serotec, Raleigh, NC, USA), PE-labeled anti-mouse Gr-1 (Miltenyi Biotec), and allophycocyanin-labeled anti-mouse CD11b (BioLegend, San Diego, CA, USA), or FITC-labeled anti-mouse CD11b (Beckman Coulter), PE-labeled anti-mouse Ly-6G (BioLegend), and allophycocyanin labeled anti-mouse Ly-6C (BioLegend) antibodies. The fluorescence intensity of the cells was measured using a FACSCalibur™ (Becton Dickinson, San Jose, CA, USA). Data obtained were visualized and analyzed using the FlowJo software (Tomy Digital Biology Co., Ltd., Tokyo, Japan).

Isolation of CD11b$^+$Gr-1$^+$ hepatic inflammatory cells and T-cell [3H]-thymidine incorporation assay

C57BL/6J female mice were injected with 300 μg of ConA and then injected with 1×10^5 ADSCs after 3 h ($n = 3$). Three

Figure 5. Immunohistochemical analysis of inflammatory cells in the liver of ConA-induced hepatitis mice treated with ADSCs. (A–C) Immunohistochemical staining of the liver. C57BL/6 female mice were injected i.v. with 300 μg of ConA. Then, 3 h later, the mice were injected with ADSCs via the tail vein. Liver tissues were obtained at (A) 6, (B)12, or (C) 24 h after ConA injection ($n = 4$ per each time point). Immunohistochemical staining was conducted using anti-CD4, anti-CD11b, anti-Gr-1, and anti-F4/80 antibodies. Stained liver images shown are representative of three experiments performed. Magnification: ×100. Bars: 200 μm. (D) Quantification of CD4$^+$, CD11b$^+$, Gr-1$^+$, and F4/80$^+$ cells in four visual fields per ×100 low-power field in the liver of representative mice from each group. Data are shown as mean +SE ($n = 4$) and are representative of three experiments performed. $^*p < 0.05$, $^{**}p < 0.01$, $^{***}p < 0.005$, $^{****}p < 0.001$; Student's *t*-test. n.s.: not significant.

hours later, hepatic inflammatory cells were isolated and incubated with FITC-labeled anti-mouse CD11b (Beckman Coulter) and PE-labeled anti-mouse Gr-1 (Miltenyi Biotec) antibodies. The $CD11b^+Gr\text{-}1^+$ population was collected using a FACSAira II™ (Becton Dickinson). $CD11b^+Gr\text{-}1^+$ cells (1×10^5), which had been irradiated with 2000 rads, were co-cultured with 1×10^5 purified splenic T cells isolated from C57BL/6J mice in RPMI1640 medium (Invitrogen) supplemented with 10% heat-inactivated FBS, 1% antibiotic–antimycotic solution (Life Technologies), and ConA (4 μg/mL) for 48 h ($n = 4$). The culture was pulsed with [3H]thymidine (1 μCi/well) for 16 h and harvested. Thymidine incorporation was measured using a beta-counter (PerkinElmer, Waltham, MA, USA).

NO assay

C57BL/6J female mice were injected with 300 μg of ConA. Three hours later, 1×10^5 ADSCs were injected via the tail vein. After a further 3 h, hepatic inflammatory cells were isolated from ConA hepatitis mice with or without ADSC treatment ($n = 3$ each) and incubated in PBS supplemented with 2% BSA, PE-labeled anti-mouse Gr-1 antibody, and allophycocyanin-labeled anti-mouse CD11b antibody. Cells were then incubated in PBS containing 2.5 mg/mL diaminofluorescein-FM diacetate (Sekisui Medical Co., Ltd., Tokyo, Japan), which emits fluorescence at 515 nm in a reaction with NO, at 37°C for 30 min and subjected to FACS analysis using a FACSCalibur flow cytometer.

Arginase assay

Female C57BL/6J mice were injected with 300 μg of ConA. Three hours later, 1×10^5 ADSCs were injected via the tail vein. After further 3 h, hepatic inflammatory cells were isolated from ConA hepatitis mice with or without ADSC treatment ($n = 3$ each) and were lysed with PBS containing 10 mM Tris-HCl (pH 7.4) and 0.4% Triton X-100, supplemented with the proteinase inhibitor cocktail, cOmplete, Mini, EDTA-free® (Roche, Basel, Switzerland). One hundred micrograms of the lysis aliquot obtained were subject to an arginase activity assay using a QuantiChrom™ Arginase Assay kit (BioAssay Systems, Hayward, CA), which measures urea produced from the substrate, in accordance with the manufacturer's protocol.

Statistical analysis

All data are expressed as means ± SE. Statistical analyses were performed using the JMP software (ver.9.02; SAS Institute Japan Inc., Tokyo, Japan). Student's *t*-test and Wilcoxon signed-rank test were used. p values < 0.05 were considered to indicate statistical significance.

Acknowledgements: This study was supported, in part, by subsidies from the Japanese Ministry of Education, Culture, Sports, Science, and Technology and the Japanese Ministry of Health, Labor, and Welfare.

Conflict of interest: The authors declare no financial or commercial conflict of interest.

References

1 **Zuk, P. A., Zhu, M., Ashjian, P., De Ugarte, D. A., Huang, J. I., Mizuno, H., Alfonso, Z. C. et al.**, Human adipose tissue is a source of multipotent stem cells. *Mol. Biol. Cell* 2002. **13**: 4279–4295.

2 **Chamberlain, G., Fox, J., Ashton, B. and Middleton, J.**, Concise review: mesenchymal stem cells: their phenotype, differentiation capacity, immunological features, and potential for homing. *Stem Cells* 2007. **25**: 2739–2749.

3 **Perez-Cano, R., Vranckx, J. J., Lasso, J. M., Calabrese, C., Merck, B., Milstein, A. M., Sassoon, E. et al.**, Prospective trial of adipose-derived regenerative cell (ADRC)-enriched fat grafting for partial mastectomy defects: the RESTORE-2 trial. *Eur. J. Surg. Oncol.* 2012. **38**: 382–389.

4 **Janssens, S.**, Stem cells in the treatment of heart disease. *Annu. Rev. Med.* 2010. **61**: 287–300.

5 **Hoogduijn, M. J., Popp, F., Verbeek, R., Masoodi, M., Nicolaou, A., Baan, C. and Dahlke, M. H.**, The immunomodulatory properties of mesenchymal stem cells and their use for immunotherapy. *Int. Immunopharmacol.* 2010. **10**: 1496–1500.

6 **Baroni, G. S., Pastorelli, A., Manzin, A., Benedetti, A., Marucci, L., Solforosi, L., Di Sario, A. et al.**, Hepatic stellate cell activation and liver fibrosis are associated with necroinflammatory injury and Th1-like response in chronic hepatitis C. *Liver* 1999. **19**: 212–219.

7 **Cerny, A. and Chisari, F. V.**, Pathogenesis of chronic hepatitis C: immunological features of hepatic injury and viral persistence. *Hepatology* 1999. **30**: 595–601.

8 **Gershwin, M. E., Ansari, A. A., Mackay, I. R., Nakanuma, Y., Nishio, A., Rowley, M. J. and Coppel, R. L.**, Primary biliary cirrhosis: an orchestrated immune response against epithelial cells. *Immunol. Rev.* 2000. **174**: 210–225.

9 **Krawitt, E. L.**, Autoimmune hepatitis. *N. Engl. J. Med.* 1996. **334**: 897–903.

10 **Fujii, H. and Kawada, N.**, Inflammation and fibrogenesis in steatohepatitis. *J. Gastroenterol.* 2012. **47**: 215–225.

11 **Dienes, H. P. and Drebber, U.**, Pathology of immune-mediated liver injury. *Dig. Dis.* 2010. **28**: 57–62.

12 **Dai, L. J., Li, H. Y., Guan, L. X., Ritchie, G. and Zhou, J. X.**, The therapeutic potential of bone marrow-derived mesenchymal stem cells on hepatic cirrhosis. *Stem Cell Res.* 2009. **2**: 16–25.

13 **Sanders, D. A., Moothoo, D. N., Raftery, J., Howard, A. J., Helliwell, J. R. and Naismith, J. H.**, The 1.2 A resolution structure of the Con A-dimannose complex. *J. Mol. Biol.* 2001. **310**: 875–884.

14 **Kato, M., Ikeda, N., Matsushita, E., Kaneko, S. and Kobayashi, K.**, Involvement of IL-10, an anti-inflammatory cytokine in murine liver injury induced by concanavalin A. *Hepatol. Res.* 2001. **20**: 232–243.

15 **Kubo, N., Narumi, S., Kijima, H., Mizukami, H., Yagihashi, S., Hakamada, K. and Nakane, A.**, Efficacy of adipose tissue-derived mesenchymal stem cells for fulminant hepatitis in mice induced by concanavalin A. *J. Gastroenterol. Hepatol.* 2012. **27**: 165–172.

16 **Murdoch, C., Muthana, M., Coffelt, S. B. and Lewis, C. E.**, The role of myeloid cells in the promotion of tumour angiogenesis. *Nat. Rev. Cancer* 2008. **8**: 618–631.

17 **Banas, A., Teratani, T., Yamamoto, Y., Tokuhara, M., Takeshita, F., Quinn, G., Okochi, H. et al.**, Adipose tissue-derived mesenchymal stem cells as a source of human hepatocytes. *Hepatology* 2007. **46**: 219–228.

18 **Kaneko, Y., Harada, M., Kawano, T., Yamashita, M., Shibata, Y., Gejyo, F., Nakayama, T. et al.**, Augmentation of Valpha14 NKT cell-mediated cytotoxicity by interleukin 4 in an autocrine mechanism resulting in the development of concanavalin A-induced hepatitis. *J. Exp. Med.* 2000. **191**: 105–114.

19 **Tiegs, G., Hentschel, J. and Wendel, A.**, A T cell-dependent experimental liver injury in mice inducible by concanavalin A. *J. Clin. Invest.* 1992. **90**: 196–203.

20 **Halder, R. C., Aguilera, C., Maricic, I. and Kumar, V.**, Type II NKT cell-mediated anergy induction in type I NKT cells prevents inflammatory liver disease. *J. Clin. Invest.* 2007. **117**: 2302–2312.

21 **Schwabe, R. F. and Brenner, D. A.**, Mechanisms of liver injury. I. TNF-alpha-induced liver injury: role of IKK, JNK, and ROS pathways. *Am. J. Physiol. Gastrointest. Liver Physiol.* 2006. **290**: G583–G589.

22 **Schumann, J., Wolf, D., Pahl, A., Brune, K., Papadopoulos, T., van Rooijen, N. and Tiegs, G.**, Importance of Kupffer cells for T-cell-dependent liver injury in mice. *Am. J. Pathol.* 2000. **157**: 1671–1683.

23 **Clegg, C. H., Rulffes, J. T., Wallace, P. M. and Haugen, H. S.**, Regulation of an extrathymic T-cell development pathway by oncostatin M. *Nature* 1996. **384**: 261–263.

24 **Constant, S. L. and Bottomly, K.**, Induction of Th1 and Th2 CD4+ T cell responses: the alternative approaches. *Annu. Rev. Immunol.* 1997. **15**: 297–322.

25 **Contento, R. L., Molon, B., Boularan, C., Pozzan, T., Manes, S., Marullo, S. and Viola, A.**, CXCR4-CCR5: a couple modulating T cell functions. *Proc. Natl. Acad. Sci. USA* 2008. **105**: 10101–10106.

26 **Ponte, A. L., Marais, E., Gallay, N., Langonne, A., Delorme, B., Herault, O., Charbord, P. et al.**, The in vitro migration capacity of human bone marrow mesenchymal stem cells: comparison of chemokine and growth factor chemotactic activities. *Stem Cells* 2007. **25**: 1737–1745.

27 **Kushiyama, T., Oda, T., Yamada, M., Higashi, K., Yamamoto, K., Oshima, N., Sakurai, Y. et al.**, Effects of liposome-encapsulated clodronate on chlorhexidine gluconate-induced peritoneal fibrosis in rats. *Nephrol. Dial. Transplant.* 2011. **26**: 3143–3154.

Abbreviations: **ADSC**: adipose tissue derived stromal stem cell · **ALT**: alanine transferase · **LDH**: lactate dehydrogenase · **MDSC**: myeloid-derived suppressor cell · **MSC**: mesenchymal stromal stem cell

Full correspondence: Dr. Shuichi Kaneko, Disease Control and Homeostasis, Kanazawa University, 13-1 Takara-machi, Kanazawa, Ishikawa 920-8641, Japan
Fax: +81-76-234-4250
e-mail: skaneko@m-kanazwa.jp

Received: 17/3/2013
Revised: 3/7/2013
Accepted: 6/8/2013
Accepted article online: 12/8/2013

HEPATOLOGY
Official Journal of the American Association for the Study of Liver Diseases

LIVER INJURY/REGENERATION

Adipose Tissue-Derived Stem Cells as a Regenerative Therapy for a Mouse Steatohepatitis-Induced Cirrhosis Model

Akihiro Seki,[1,2*] Yoshio Sakai,[1,3*] Takuya Komura,[2] Alessandro Nasti,[2] Keiko Yoshida,[2] Mami Higashimoto,[2] Masao Honda,[1] Soichiro Usui,[2] Masayuki Takamura,[2] Toshinari Takamura,[2] Takahiro Ochiya,[4] Kengo Furuichi,[5] Takashi Wada,[3] and Shuichi Kaneko[1,2]

Cirrhosis is a chronic liver disease that impairs hepatic function and causes advanced fibrosis. Mesenchymal stem cells have gained recent popularity as a regenerative therapy since they possess immunomodulatory functions. We found that injected adipose tissue-derived stem cells (ADSCs) reside in the liver. Injection of ADSCs also restores albumin expression in hepatic parenchymal cells and ameliorates fibrosis in a nonalcoholic steatohepatitis model of cirrhosis in mice. Gene expression analysis of the liver identifies up- and down-regulation of genes, indicating regeneration/repair and anti-inflammatory processes following ADSC injection. ADSC treatment also decreases the number of intrahepatic infiltrating CD11b$^+$ and Gr-1$^+$ cells and reduces the ratio of CD8$^+$/CD4$^+$ cells in hepatic inflammatory cells. This is consistent with down-regulation of genes in hepatic inflammatory cells related to antigen presentation and helper T-cell activation. *Conclusion*: These results suggest that ADSC therapy is beneficial in cirrhosis, as it can repair and restore the function of the impaired liver. (HEPATOLOGY 2013;58:1133-1142)

Cirrhosis is a serious, life-threatening advanced stage of chronic liver disease that leads to hepatic dysfunction.[1] Cirrhosis frequently develops into hepatocellular carcinoma,[2,3] which exacerbates the prognosis of patients with cirrhosis. The ultimate treatment for cirrhosis is a liver transplant,[4] which can be lethal.[5] The number of donor livers, however, is not sufficient to meet the needs of all transplant patients. Thus, a novel therapy for cirrhosis needs to be developed to improve cirrhotic liver prognosis.

The underlying pathogenesis of chronic liver disease is persistent inflammation. Advanced disease is marked by advanced fibrosis concomitant with distorted liver architecture characterized by regenerative nodules and impaired hepatic function. Advanced fibrosis in the cirrhotic liver is also a risk factor for the development of hepatocellular carcinoma.[6] Treatment of cirrhosis suppresses inflammation by eradicating hepatitis virus infection or reducing liver steatosis in nonalcoholic steatohepatitis (NASH). Decreasing liver inflammation and restoring hepatocyte function improves the prognosis.

Pluripotent mesenchymal stem cells (MSCs) differentiate into adipocyte, chondrocyte, and osteocyte lineages.[7] These cells can also differentiate into other lineages, including neurons[8] and hepatocytes.[9,10] MSCs can also regulate the immune response.[11] Thus, MSCs attract attention as a therapeutic target in the

Abbreviations: ADSCs, adipose-tissue-derived stem cells; AFP, alpha-fetoprotein; Ath+HF, atherogenic high-fat; IL, interleukin; MMP, matrix metalloproteinase; MSC, mesenchymal stem cells; NASH, nonalcoholic steatohepatitis; PBS, phosphate-buffered saline; 18S rRNA, 18S ribosomal RNA; α-SMA, alpha-smooth muscle actin.

From the [1]Department of Gastroenterology, Kanazawa University Hospital, Ishikawa, Japan; [2]Disease Control and Homeostasis, Kanazawa University, Ishikawa, Japan; [3]Department of Laboratory Medicine, Kanazawa University Hospital, Ishikawa, Japan; [4]National Cancer Research Institute, Tokyo, Japan; [5]Division of Blood Purification, Kanazawa University Hospital, Ishikawa, Japan.

Received September 27, 2012; accepted April 15, 2013.

Supported in part by subsidies from the Japanese Ministry of Education, Culture, Sports, Science and Technology and the Japanese Ministry of Health, Labor and Welfare.

**These authors contributed equally to this work.*

regeneration or repair of various impaired organs. Mesenchymal tissue from bone marrow, umbilical cord, and adipose tissue are relatively enriched with pluripotent stem cells.[12] Since the pathophysiological features of liver cirrhosis are a consequence of chronic hepatic inflammation, MSCs are especially suited to enhance regeneration and/or repair of damaged cirrhotic liver.

We have established a clinically relevant NASH cirrhotic murine model by feeding animals an atherogenic high-fat (Ath+HF) diet.[13] In this study we examined whether adipose-tissue-derived stem cells (ADSCs) can regenerate and/or repair the cirrhotic liver. We observed that injected ADSCs resided in the liver and expressed albumin, leading to restored albumin expression in hepatic parenchymal cells. ADSCs also ameliorated advanced fibrosis. Moreover, ADSCs suppressed the underlying persistent inflammation contributed by granulocytes, phagocytic cells, and T cells. These results suggest that treatment of patients with cirrhosis with ADSCs is a potentially novel approach for regenerating and/or repairing damaged cirrhotic liver tissue to restore hepatic function.

Materials and Methods

Culture of ADSCs. ADSCs were prepared as described.[14] Briefly, adipose tissue was obtained from the inguinal subcutaneous region of 10-week-old GFP-Tg male mice (a gift from Professor Okabe, Osaka University, Japan). The stem cell fraction was isolated from adipose tissue using type-I collagenase (Wako Pure Chemical Industries, Osaka, Japan) and cultured in Dulbecco's modified Eagle's medium: nutrient mixture F-12 supplemented with 10% heat-inactivated bovine serum albumin and 1% antibiotic-antimycotic solution. Cell culture reagents were purchased from Life Technologies (Carlsbad, CA).

NASH Murine Model. Female 8-week-old C57Bl/6J mice were purchased from Charles River Laboratories Japan (Yokohama, Japan). Mice were fed an Ath+HF diet composed of cocoa butter, cholesterol, cholate, and corticotropin-releasing factor-1 (Oriental Yeast Co., Tokyo, Japan) to induce steatohepatitis as reported previously.[13] Our Institutional Review Board approved the care and use of laboratory animals in all experiments.

ADSC Treatment of NASH Mice. ADSCs were harvested after six to eight passages in culture by treatment with trypsin/EDTA (Life Technologies) and passed through a 100-μm Cell Strainer mesh (BD Biosciences, San Jose, CA). Laparotomy was performed to inject 1×10^5 ADSCs or phosphate-buffered saline (PBS) into the splenic subcapsule. After ADSC treatment, the mice were anesthetized with pentobarbital (40 mg/kg; Kyoritsu Seiyaku, Tokyo, Japan), after which the liver was perfused with PBS and dissected. A portion of liver tissue was homogenized and incubated with type I collagenase (Wako Pure Chemical Industries), and hepatic parenchymal cells and inflammatory cells were separated with Percoll (GE Healthcare UK, Buckinghamshire, UK). $CD4^+$ T cells were isolated from hepatic inflammatory cells using a magnetic sorting system, the $CD4^+$ T cell Isolation Kit II (Miltenyi Biotec, Gladbach, Germany).

Histology and Immunohistochemical Staining. Liver tissue was preserved with formalin for paraffin embedding or embedded in OCT compound and frozen for sectioning (Sakura Finetek Japan, Tokyo, Japan). The frozen liver sections were fixed in acetone and endogenous peroxidase activity blocked with 3% hydrogen peroxide solution. After washing in PBS, the sections were incubated with a rabbit anti-CD11b antibody (BD Pharmingen, San Diego, CA) and a rabbit anti-Gr-1 antibody (eBioscience, San Diego, CA) overnight at 4°C. The slides were then washed and incubated with Histofine mouse MAXPO (Nichirei Bioscience, Tokyo, Japan) for 1 hour at room temperature. The immune complex was visualized by incubating with diaminobenzidine for 5 minutes. The paraffin-embedded sections were stained with a rabbit-anti-GFP antibody (Millipore, Billerica, MA), a rabbit anti-α-smooth muscle actin (α-SMA) antibody (Abcam, Cambridge, UK), and a rabbit anticollagen IV antibody (Abcam). Secondary antibody development was performed with diaminobenzidine as described above. In some experiments, the sliced

Address reprint requests to: Shuichi Kaneko, 13-1 Takara-machi, Kanazawa, Ishikawa 920-8641, Japan. E-mail: skaneko@m-kanazawa.jp; fax: +81-76-234-4250.

View this article online at wileyonlinelibrary.com.
DOI 10.1002/hep.26470
Potential conflict of interest: Nothing to report.
Additional Supporting Information may be found in the online version of this article.

sections were double-stained with a combination of a goat antimouse serum albumin antibody (Abcam) and a rabbit anti-GFP antibody followed by the secondary antibody and development as described above. To quantify fibrosis, paraffin-embedded sections were stained with Azan and viewed microscopically, after which the stained area was calculated using an image-analysis system (BIOREVO BZ-9000 and BZ-H1C, Keyence Japan, Osaka, Japan).

Flow Cytometry. Isolated hepatic inflammatory cells were incubated in PBS supplemented with 2% bovine serum albumin (Sigma-Aldrich, St. Louis, MO) for 10 minutes at 4°C. The cells were incubated with fluorescein isothiocyanate (FITC)-conjugated anti-CD4 (eBioscience) and phycoerythrin (PE)-conjugated anti-CD8 antibodies (eBioscience) for 30 minutes at 4°C before examination using a FACSCalibur cytometer (BD Biosciences). Similarly, ADSCs were incubated with PE-conjugated CD90 (Beckman Coulter, Fullerton, CA), or PE-conjugated CD105 (Miltenyi Biotec). The data were analyzed using the FlowJo software (Tree Star, Ashland, OR).

DNA Microarray Analysis. Isolated RNAs were amplified and labeled with Cy3 using a QuickAmp Labeling Kit (Agilent Technologies, Santa Clara, CA) in accordance with the manufacturer's protocol. cRNA (825 ng) was hybridized onto a Whole Mouse Genome 4 × 44K Array (Agilent Technologies). The hybridized microarray slide was scanned using a DNA microarray scanner (model G2505B; Agilent Technologies).

Gene expression analysis was carried out using GeneSpring analysis software (Agilent Technologies). Each measurement was divided by the 75th percentile of all measurements in that sample to normalize per chip. Hierarchical clustering and principal component analysis of gene expression was performed. Welch's t test with Benjamini and Hochberg's false-discovery rate were used to identify differentially expressed genes in the groups of interest. Analysis of biological processes was performed using the MetaCore software suite (GeneGo, San Diego, CA). BRB array tools (http://linus.nci.nih.gov/BRB-ArrayTools.html) were also used for unsupervised clustering or one-way clustering analysis. Microarray data were deposited in the NBCI Gene Expression Omnibus (GSE ID: GSE40395).

Statistical Analysis. GraphPad Prism (v. 5.0; GraphPad Software, La Jolla, CA) was used to perform a Mann-Whitney U test to compare data between two groups, and differences were considered statistically significant at $P < 0.05$.

All other materials and methods are described in the Supporting Information.

Results

Characteristics of the NASH Mouse Model. The pathological and clinical features of cirrhosis in patients are not well replicated by the majority of chemically induced murine cirrhotic liver models. We have established steatohepatitis as a cirrhotic liver mouse model by feeding mice an Ath+HF diet.[13] When mice were fed this diet for 34 weeks, hepatocytes developed steatosis, Mallory-Denk bodies, and ballooning (Fig. 1A,B), which are identical to typical pathological features of clinical NASH.[15] Albumin expression in parenchymal cells of the cirrhotic liver significantly decreased in mice fed the Ath+HF diet for 24 weeks (Fig. 1C), while alpha-fetoprotein (AFP) expression was not affected (Fig. 1D). Fibrosis developed and reached maximal levels after 34 weeks of feeding the Ath+HF diet (Fig. 1E,F). Immunohistochemical staining for immunomodulatory cells showed an increased number of Gr-1$^+$ cells in the liver of the steatohepatitis mice fed the Ath+HF diet for 12, 34, and 70 weeks (Fig. 2A,B). The number of CD11b$^+$ cells in the liver also increased and reached maximal levels after 34 weeks of feeding the Ath+HF diet (Fig. 2C,D). Thus, the murine cirrhosis model established by an Ath+HF diet mimics the features of clinical NASH.

Effect of ADSCs Treatment on Liver Albumin Expression and Fibrosis. Adipose tissue contains MSCs, which have the potential to differentiate into several types of cell lineages[10,14] and to act as immunomodulators.[11] In this study, we isolated stromal cells from inguinal adipose tissue of GFP-expressing transgenic (GFP-Tg) mice as ADSCs and expanded them in culture. The majority of these cells expressed CD90 and CD44, known surface markers of mesenchymal cells (Supporting Fig. 1A). A proportion of the expanded ADSCs also expressed CD105 (Supporting Fig. 1B), which has been recognized as a representative surface marker of MSCs.[11]

We evaluated whether ADSCs could provide a therapeutically beneficial treatment for liver cirrhosis in steatohepatitis mice. We injected 1 × 10^5 GFP-ADSCs by way of the spleen/portal vein in mice fed the Ath+HF diet for 32 weeks. We observed that the GFP-ADSCs resided in all lobes of the liver at 3, 7, and 14 days after injection (Fig. 3A,B). Importantly, immunohistochemical staining showed that GFP$^+$ cells in the cirrhotic liver expressed higher levels of albumin than did the surrounding parenchymal cells (Fig. 3C).

We also injected 1 × 10^5 or 2 × 10^4 GFP-ADSCs twice every 2 weeks by way of the splenic/portal vein

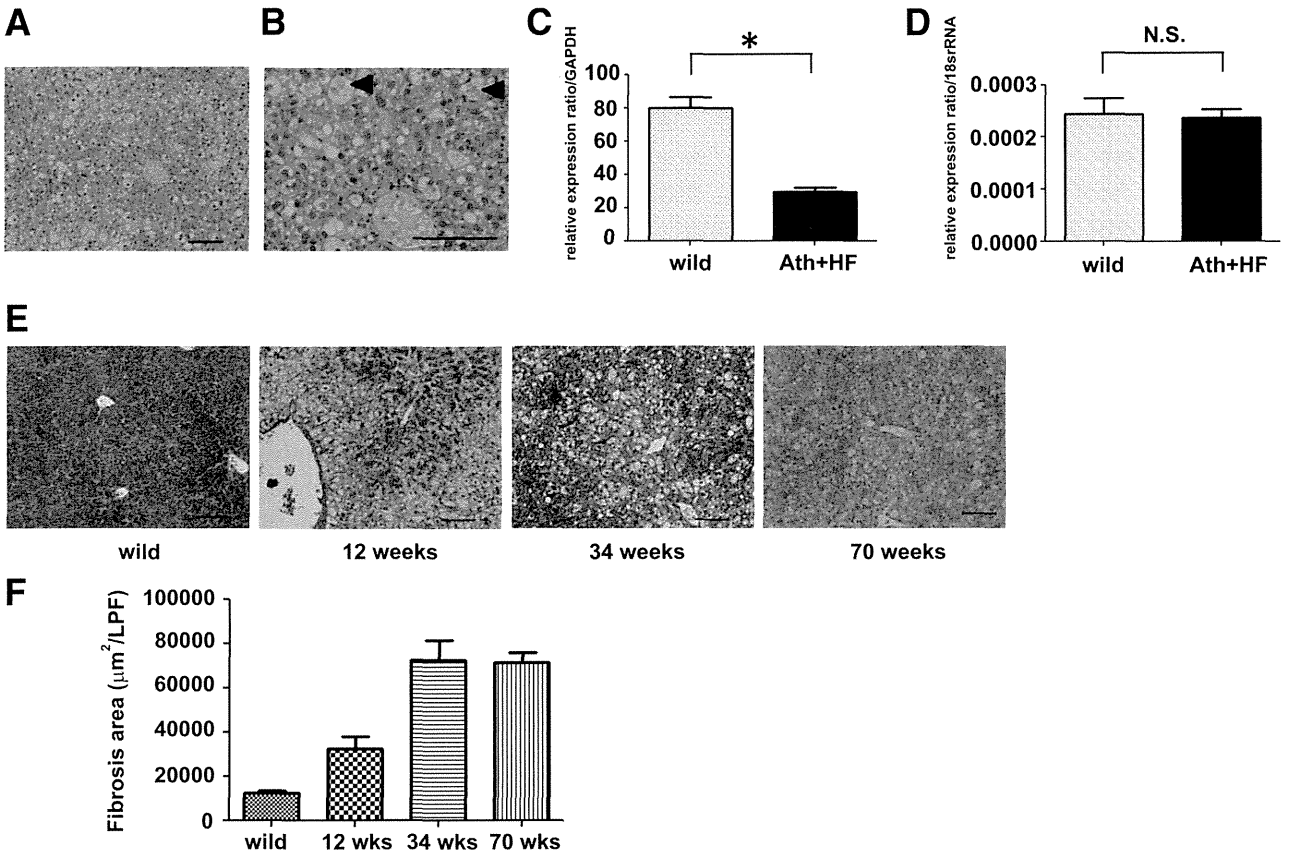

Fig. 1. Characteristics of the steatohepatitis murine model. Eight-week-old C57Bl/6 female mice were fed an Ath+HF diet. Liver tissue was obtained after 34 weeks, sectioned, and histologically examined with hematoxylin and eosin staining in (A,B) mice fed an Ath+HF diet for 34 weeks. Arrowheads indicate a Mallory-Denk body in a hepatocyte with ballooning. Parenchymal cells were isolated from 32-week-old C57Bl/6 wild-type female mice or Ath+HF mice that started the diet at 8 weeks old and continued for 24 weeks. Expression of (C) albumin and (D) AFP was assessed by reverse-transcription polymerase chain reaction (RT-PCR), n = 4, $*P < 0.05$. (E) Fibrosis was histologically examined with Azan staining in liver tissue of mice fed the Ath+HF diet for 12, 34, and 70 weeks. (F) Fibrosis areas of mice at 12, 34, and 70 weeks per ×100 low-power field were calculated for five visual fields. Bars: standard error. Scale bars = 100 μm.

in mice fed an Ath+HF diet for 32 or 36 weeks, respectively. Two weeks after the last injection the mice were euthanized and the therapeutic effects were assessed. The expression of albumin (Fig. 4A) was restored in hepatic parenchymal cells of cirrhotic mice at 2 weeks after the last injection, suggesting that ADSC treatment restored parenchymal cell function. The expression of AFP was also increased by ADSC treatment (Fig. 4B), implying enhanced regeneration of hepatic parenchymal cells. Similar effects were observed with a reduced number of (2×10^4) GFP-ADSCs (Supporting Fig. 2A,B).

We also assessed the effect of ADSC injection on fibrosis in cirrhotic mice. Liver tissue stained with Azan and anticollagen type IV antibody showed that ADSC administration reduced fibrosis compared to control animals (Fig. 5A,B; Supporting Fig. S3A,B). We also evaluated immunohistochemical staining of α-SMA, a marker of stellate cells, which are largely responsible for developing fibrosis. These results demonstrated that the number of α-SMA$^+$ cells was reduced by ADSC treatment (Fig. 5C-E), suggesting that ADSCs suppress the activity of stellate cells and ameliorate liver fibrosis.

Gene Expression Profiling of Cirrhotic Livers Following ADSC Treatment. We examined the gene expression profile of the livers in the NASH mouse model of cirrhosis by DNA microarray to determine whether administration of ADSCs was therapeutically beneficial. We identified expression of 1,249 gene probes that were significantly affected by ADSC injection. Clustering analysis of gene expression using these gene probes distinguished between ADSCs-treated mice and PBS-treated mice (Fig. 6A). Among 1,249 genes, 797 were up-regulated and 452 were down-regulated by ADSC treatment. Regarding matrix metalloproteinase (MMP), expressions of MMP-8 and MMP-9 were enhanced in the liver of NASH mice treated with PBS compared to the wild type; this enhancement was removed by ADSC treatment

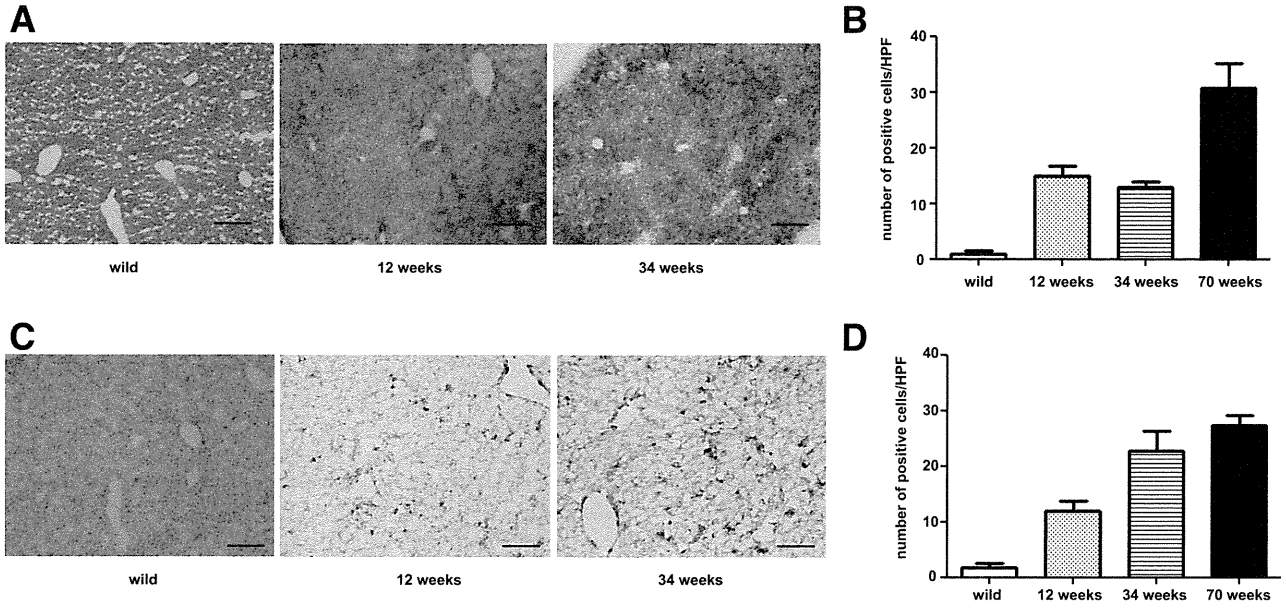

Fig. 2. Immunohistochemical staining of a steatohepatitis liver. Eight-week-old female C57Bl/6 female mice were fed an Ath+HF diet. Liver tissue was obtained from these mice or from wild-type animals after 12, 34, and 70 weeks. Immunohistochemical staining was performed for (A) Gr-1^+ or (C) $CD11b^+$ cells and the number of positive cells in a high-power field was counted for five visual fields for (B) Gr-1 or (D) CD11b at each timepoint.

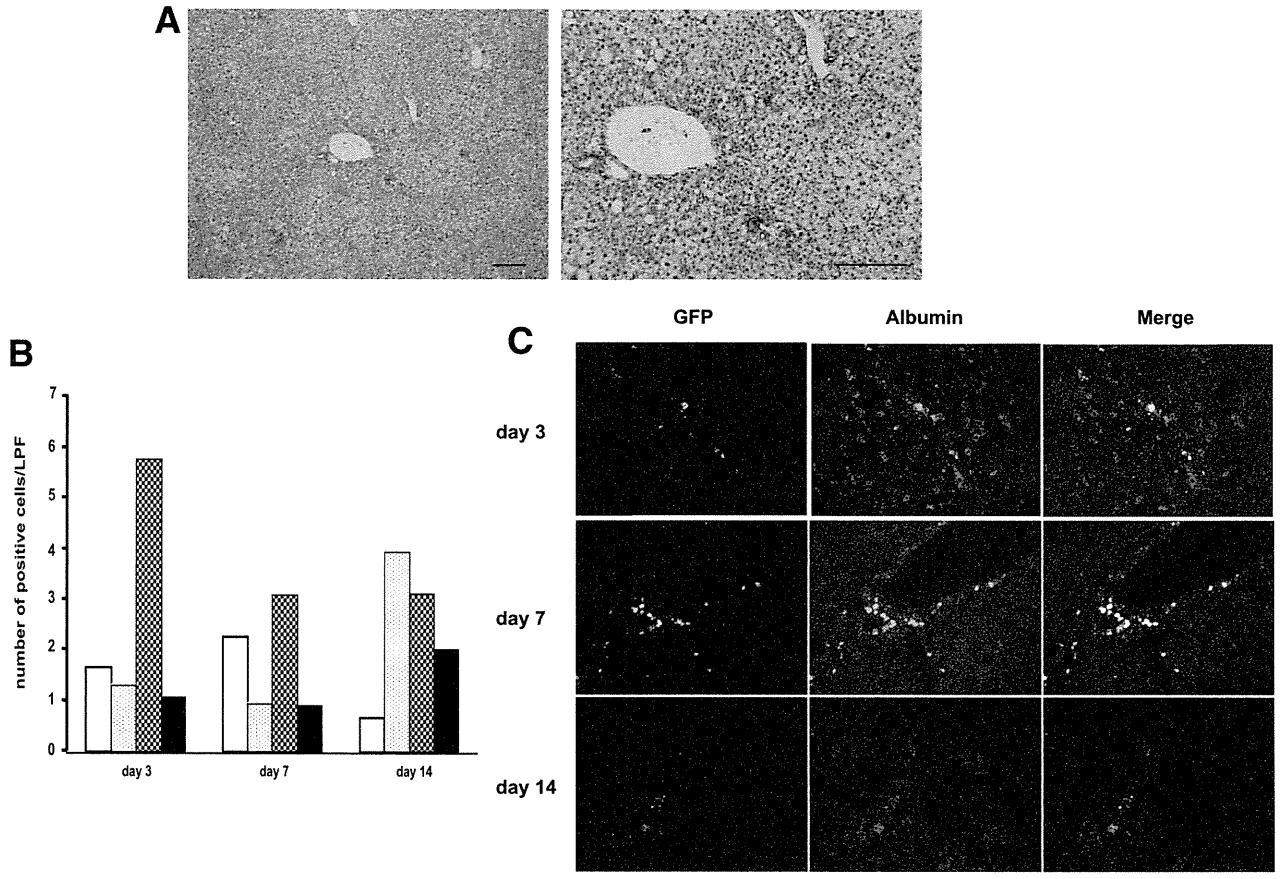

Fig. 3. Distribution of ADSCs and albumin expression in the livers of steatohepatitis mice. ADSCs from GFP-Tg mice (1×10^5) were injected into the splenic subcapsule of cirrhotic C57Bl/6 mice fed the Ath+HF diet for 32 weeks. After 3, 7, and 14 days, liver tissue was obtained and examined by immunohistochemical staining for (A) GFP; Scale bars = 100 μm. (B) GFP^+ cells in the liver were counted per ×100 low-power field and five visual fields were calculated. White bar, caudate lobe; dotted bar, left lobe; hatched bar, middle lobe; black bar, right lobe. (C) Immunohistochemical staining for GFP or albumin antibody. Magnification, ×100.

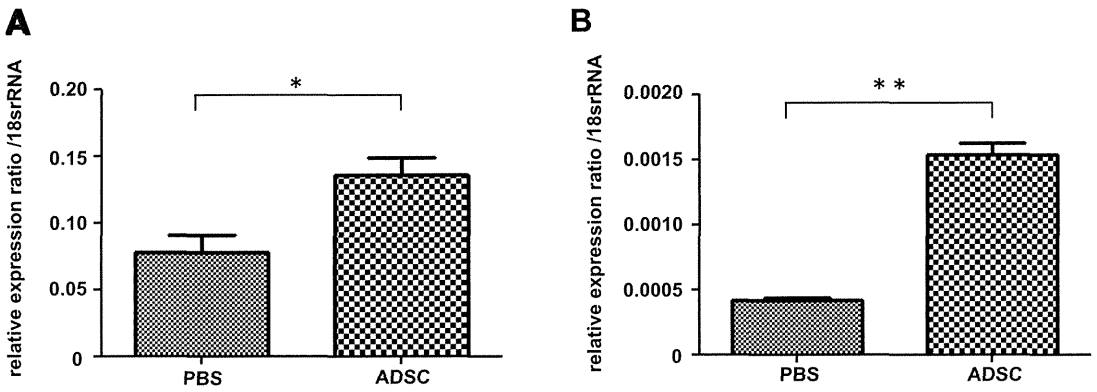

Fig. 4. Albumin and AFP expression in hepatic parenchymal cells. ADSCs from GFP-Tg mice (1×10^5) were injected twice every 2 weeks into the splenic subcapsule of cirrhotic C57Bl/6 mice fed an Ath+HF diet for 32 weeks. Control mice received PBS injections. Two weeks after the last injection, liver tissue was obtained and parenchymal cells were isolated for real-time PCR. Expressions of (A) albumin and (B) AFP were normalized relative to that of 18S ribosomal RNA (rRNA); $^*P < 0.05$, $^{**}P < 0.01$.

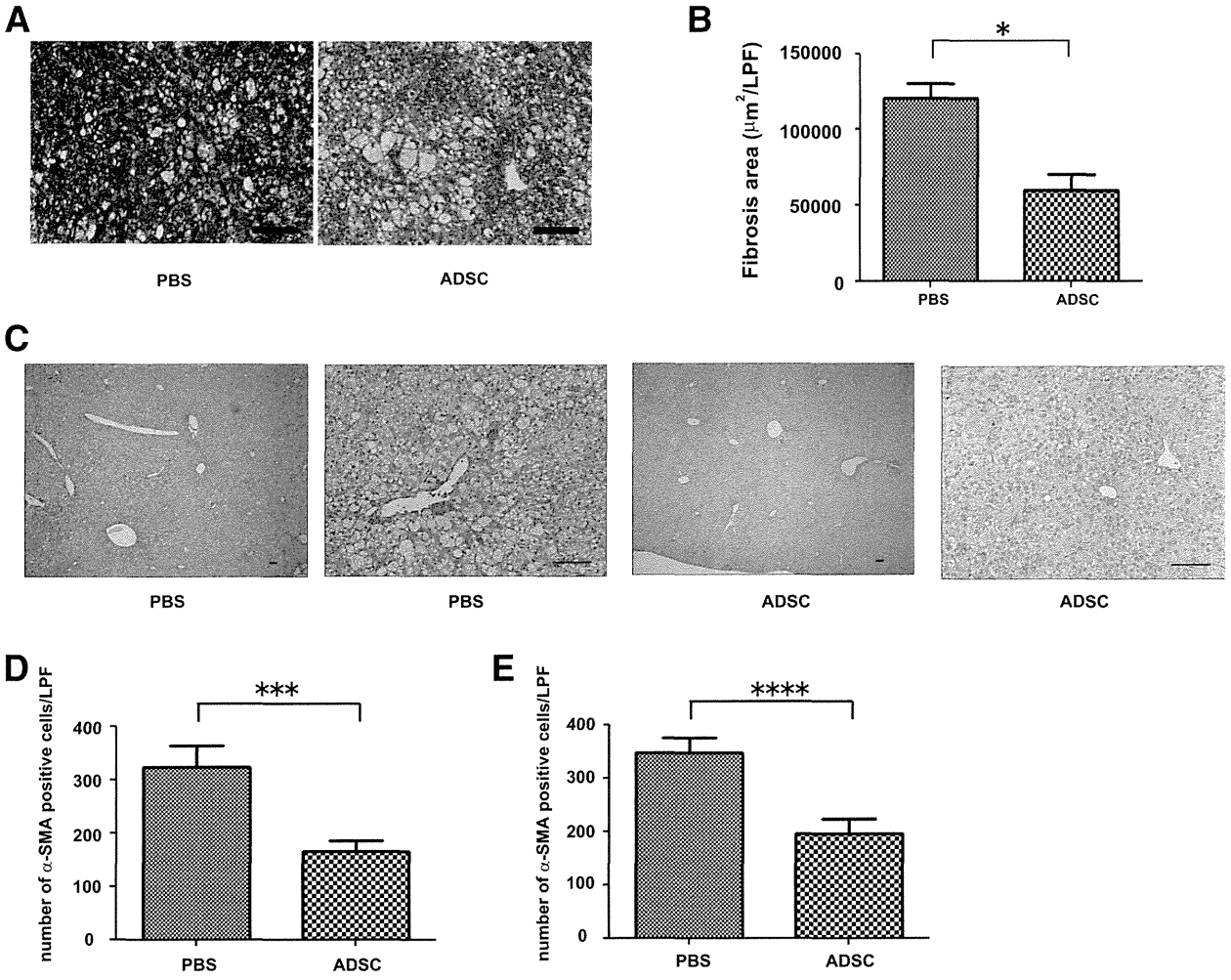

Fig. 5. Effect of ADSCs on liver fibrosis. ADSCs from GFP-Tg mice (1×10^5) were injected twice every 2 weeks into the splenic subcapsule of cirrhotic C57Bl/6 mice fed the Ath+HF diet for 32 weeks. Control mice received PBS injections. (A) Two weeks after the last injection, liver tissue was obtained, sectioned, and histologically examined with hematoxylin and eosin staining. (B) Fibrosis was examined by Azan staining and fibrotic area was quantified by image-analysis. (C) Immunohistochemical staining of liver sections for α-SMA. Scale bars = 100 μm. (D,E) The number of α-SMA+ cells in liver tissues obtained 1 (D) or 2 weeks (E) after the last ADSC injection determined by microscopy of five low-power fields (×100); $^{***}P < 0.005$, $^{****}P = 0.0001$.

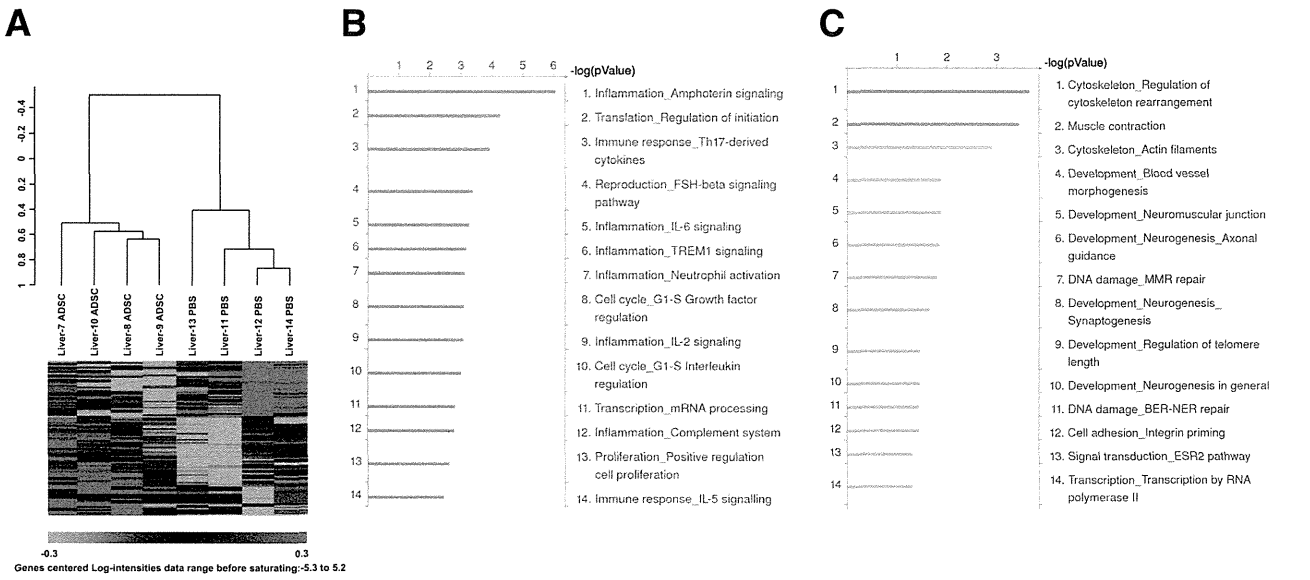

Fig. 6. Hepatic gene expression analysis. ADSCs from GFP-Tg mice (1×10^5) were injected twice every 2 weeks into the splenic subcapsule of cirrhotic C57Bl/6 mice fed an Ath+HF diet for 40 weeks. Control mice received PBS injections. Two weeks later, liver tissue was subjected to RNA isolation and gene expression using DNA microarrays. (A) Unsupervised clustering analysis was performed using probes for 1,249 genes whose expression differed significantly between the PBS and ADSC groups. (B) The biological processes of 452 genes whose expression was down-regulated in the ADSCs group compared to the PBS group were analyzed. (C) The biological processes of 797 genes whose expression was up-regulated in the ADSCs group compared to the PBS group were analyzed.

(Supporting Fig. S4). Biological process analysis indicated that the down-regulated genes were primarily related to inflammation and the immune response (Fig. 6B), and the up-regulated genes were related to tissue construction and development (Fig. 6C). Thus, gene expression analysis of liver tissue demonstrated that ADSCs treatment caused anti-inflammatory effects, as well as regeneration/repair effects, in the livers of a NASH mouse model of cirrhosis.

Anti-inflammatory Effects of ADSC Treatment. The fundamental underlying pathophysiology of steatohepatitis-induced cirrhosis is persistent hepatic inflammation caused by steatosis in hepatocytes.[16] We examined how ADSCs affected persistent inflammation of the liver in NASH mice at 2 weeks after the last injection of ADSCs. Immunohistochemical staining showed that the number of $CD11b^+$ cells accumulating in the livers of cirrhotic mice decreased with ADSC treatment compared to those of PBS-treated mice (Fig. 7A). The number of $Gr\text{-}1^+$ cells in cirrhotic liver also decreased with ADSC treatment (Fig. 7A), suggesting that ADSCs affect granulocytes and antigen-presenting cell lineage.

We further examined whether ADSC treatment affected the lymphocyte lineage of T cells, since they also play an important role in immune regulation of steatohepatitis.[17] We isolated lymphocytes from the livers of mice treated with ADSCs and examined the $CD4^+$ and $CD8^+$ T cells using flow cytometry. $CD8^+$ T cells were found predominantly in cirrhotic mice treated with PBS (Fig. 7B,C). However, when the mice were treated with ADSCs the number of $CD4^+$ T cells increased and was comparable to that of $CD8^+$ T cells, indicating that ADSC treatment affected T-cell subpopulations.

Gene Expression Profiling of Hepatic Inflammatory Cells Following ADSC Treatment. We further examined how injected ADSCs affected hepatic inflammatory cell gene expression by using DNA microarrays. By filtering the results from 5,065 gene probes, completely discernible clusters of gene expression were formed between ADSC- and PBS-treated animals (Fig. 8A). We identified the expression of 873 genes that were significantly up-regulated at least 2-fold with ADSC injection and 658 genes that were down-regulated. Most of the chemokines and cytokines whose expression was significantly affected by ADSCs were down-regulated (Supporting Table S1). Using the publicly available gene expression database for hematopoietic cells (GSE27787) and various types of helper T cells (GSE14308), we examined features of these affected genes in the context of immunomodulatory cells. Among the hematopoietic cells, genes with available symbol annotation were predominately $Gr\text{-}1^+$ and $CD11b^+$ cells from granulocyte and macrophage lineages (Fig. 8B). Among helper T-cell populations,

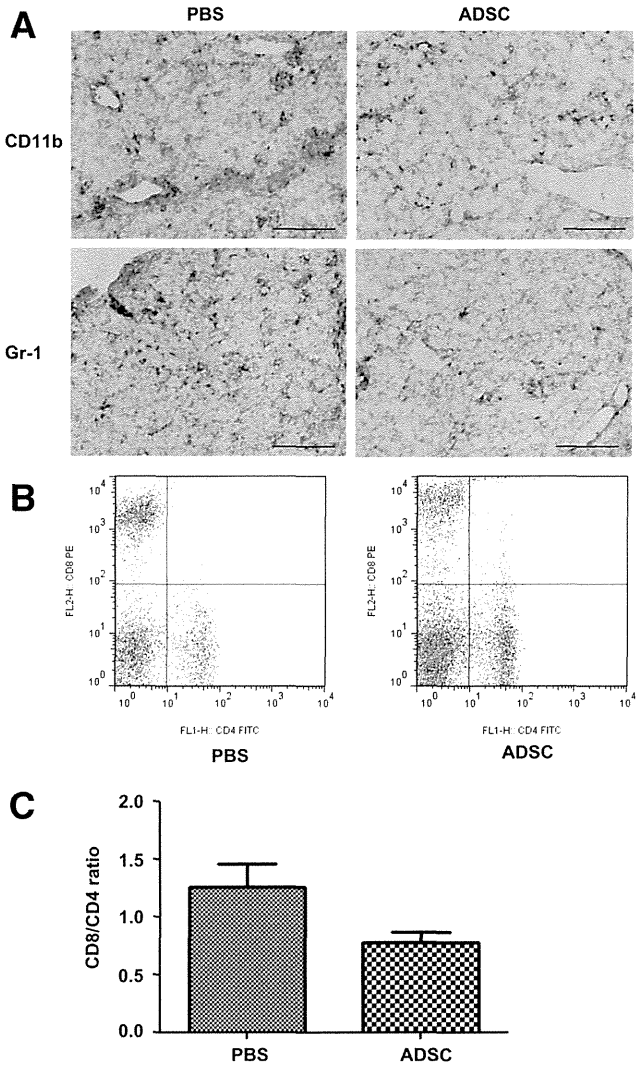

Fig. 7. Effect of ADSCs on inflammatory cells in the cirrhotic liver. ADSCs from GFP-Tg mice (1×10^5) were injected twice every 2 weeks into the splenic subcapsule of cirrhotic C57Bl/6 mice fed the Ath+HF diet for 32 weeks. Control mice received PBS injections. Two weeks later, liver tissue was obtained and immunohistochemical staining of (A) $CD11b^+$ and (B) $Gr\text{-}1^+$ cells was performed. Inflammatory cells in the liver were also isolated and stained with FITC-labeled anti-CD4 and PE-labeled CD8 antibodies. (C) The ratio of $CD8^+$ cells to $CD4^+$ cells was calculated. N = 4 ± standard error.

annotated genes included activated Th1, Th2, and Th17 cell types (Fig. 8C). We also isolated $CD4^+$T cells from hepatic inflammatory cells obtained from NASH mice fed an Ath+HF diet for 12 weeks, then treated with ADSC. Expressions of the Th1, Th2, and Th17 cytokines, interferon-γ, interleukin (IL)−4, IL-10, and IL-17, the Th17-related cytokine transforming growth factor beta (TGF-β), and Foxp3, a representative transcription factor of regulatory T cells, were down-regulated by ADSC treatment (Supporting Fig. S5).

These results suggest that ADSC treatment suppresses inflammation in the NASH mouse model primarily by down-regulating granulocytes, antigen-presenting cells, and activated helper T cells.

Discussion

This study investigated the therapeutic effect of ADSCs in a NASH murine model of cirrhosis. This model is relevant to clinical NASH, with similar pathological features established by an atherogenic high-fat diet, including the appearance of steatosis, ballooning, and Mallory-Denk bodies in hepatocytes, infiltration of inflammatory cells, and pericellular fibrosis. Our results demonstrate that ADSC injection is therapeutically beneficial for cirrhosis in this murine model through restoration of albumin expression in hepatic parenchymal cells, amelioration of fibrosis, and suppression of persistent hepatic inflammation.

Gene expression analysis of the liver in this cirrhotic mouse model revealed that ADSC injection affects biological processes relating to anti-inflammatory and regeneration/repair pathways. The anti-inflammatory effects are mediated by ADSC targeting of $Gr\text{-}1^+$, $CD11b^+$, and helper T-cell lineages. In patients with clinical NASH, the ratio of neutrophils to lymphocytes increases,[18] suggesting that granulocytes are involved in the pathogenesis of NASH. The NASH murine model used in this study produced an increased $CD8^+/CD4^+$ T-cell ratio, which is also comparable to clinical NASH patient pathology.[19] Gene expression analysis of liver tissue and hepatic inflammatory cells from NASH mice showed that Th1-, Th2-, and Th17-related genes were down-regulated by ADSC treatment. Helper T-cell activation skewed to produce Th1 cytokines is pathogenic in steatohepatitis.[20,21] In particular, Th17 is emerging as an important source of IL-17 family cytokines[22] and is involved in the hepatic inflammation in NASH.[23] Helper T cells producing Th2 cytokines such as IL-4, 5, and 13 contribute to fibrosis.[24] We conclude that activated T helper cells are responsible for the pathogenesis of steatohepatitis in the NASH murine model used in this study and that ADSCs suppress pathogenic helper T-cell activation. However, the suppression of miscellaneous effector and regulatory helper T cells by ADSCs should be further evaluated with regard to prevention of hepatocellular carcinoma, a frequent sequela to cirrhosis, since Th1 promotes antitumor immunity and Th2 down-regulates antitumor immunity.

We also observed that ADSC treatment ameliorated fibrosis and decreased the number of α-SMA^+ stellate

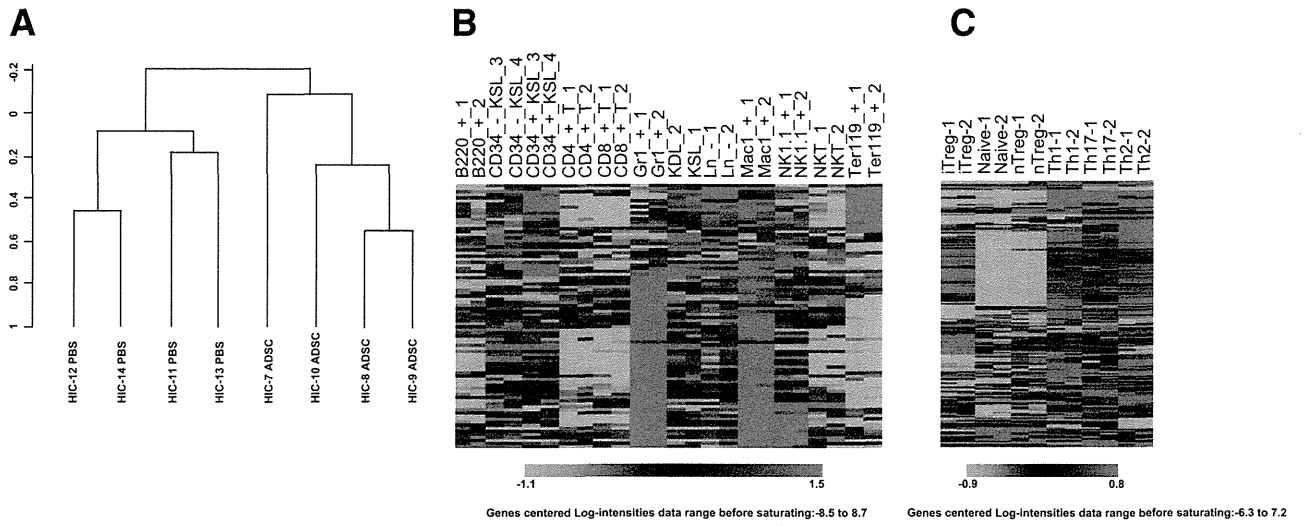

Fig. 8. Gene-expression analysis of intrahepatic inflammatory cells. ADSCs from GFP-Tg mice (1×10^5) were injected twice every 2 weeks into the splenic subcapsule of cirrhotic C57Bl/6 mice fed an Ath+HF diet for 40 weeks. Control mice received PBS injections. Inflammatory cells were isolated from the liver and gene expression examination was performed using DNA microarrays. (A) Unsupervised clustering analysis using the filtered 5,065 gene probes. HIC; hepatic inflammatory cells. (B) One-way clustering analysis using a publicly available database of hematopoietic cells (GSE27787) of 658 genes whose expression was down-regulated by ADSC treatment with available gene symbol annotations. (C) One-way clustering analysis using publicly available database of different helper T subsets (GSE14308) of 658 genes whose expression was down-regulated by ADSCs treatment with available gene symbol annotations.

cells in cirrhotic liver. When inflammation persists in the liver, fibrosis progresses due to these activated stellate cells, which are almost identical to myofibroblasts and produce extracellular matrix. Stellate cells are activated by miscellaneous factors including TGF-β and platelet-derived growth factor,[25] produced mostly from Kupffer cells. Helper T cells expressing Th2 cytokines are also involved in the development of fibrosis. Gene expression analysis of the cirrhotic livers indicated that ADSC treatment suppressed Th2-type helper T cells. Although details of how these molecules mediate fibrosis development have yet to be examined in the current NASH murine model, the antifibrotic effect of ADSCs is achieved in part by suppressing Th2-type helper T cells. We found that MMP-8 and MMP-9 enhancement in the NASH-cirrhotic liver was ameliorated by ADSC treatment. MMP-9 expression is related to the inflammation typical of steatohepatitis[26] and can ameliorate the hepatic fibrosis induced by carbon tetrachloride.[27] Further studies are needed to clarify the role of MMPs in the pathogenesis of cirrhosis as well as to explore novel therapies for this condition.

Pluripotent MSCs differentiate into several cell lineages and are a promising avenue for regenerative therapy of various impaired organs, including the liver. Although ADSCs were observed in cirrhotic livers at up to 2 weeks after injection and expressed albumin, the numbers of resident cells were not sufficient to supplement hepatic function. Therefore, pluripotency, as well as the anti-inflammatory and antifibrotic effects of ADSCs, are important for their regenerative/repair effects in liver cirrhosis. Rather than studying the effects of ADSCs on early-stage steatohepatitis, we treated mice with endstage cirrhosis with ADSCs to observe their therapeutic effects. Our results demonstrated that ADSCs can effectively resolve chronic fibrosis and decrease inflammation, thereby restoring hepatic function in endstage cirrhotic mice, implying the usefulness of this therapy as an alternative to liver transplantation.

In conclusion, ADSCs proved therapeutically beneficial and clinically relevant in regenerative therapy of a murine steatohepatitis-cirrhosis model. Clinical application of ADSCs in the treatment of cirrhosis is expected to provide a novel alternative regenerative/repair therapy for patients with cirrhosis.

References

1. D'Amico G, Garcia-Tsao G, Pagliaro L. Natural history and prognostic indicators of survival in cirrhosis: a systematic review of 118 studies. J Hepatol 2006;44:217-231.
2. Llovet JM, Burroughs A, Bruix J. Hepatocellular carcinoma. Lancet 2003;362:1907-1917.
3. Fattovich G, Stroffolini T, Zagni I, Donato F. Hepatocellular carcinoma in cirrhosis: incidence and risk factors. Gastroenterology 2004;127:S35-50.
4. Kamath PS, Kim WR. The model for end-stage liver disease (MELD). HEPATOLOGY 2007;45:797-805.
5. Stravitz RT, Carl DE, Biskobing DM. Medical management of the liver transplant recipient. Clin Liver Dis 2011;15:821-843.

6. Forner A, Llovet JM, Bruix J. Hepatocellular carcinoma. Lancet 2012;379:1245-1255.
7. Chamberlain G, Fox J, Ashton B, Middleton J. Concise review: mesenchymal stem cells: their phenotype, differentiation capacity, immunological features, and potential for homing. Stem Cells 2007;25:2739-2749.
8. Franco Lambert AP, Fraga Zandonai A, Bonatto D, Cantarelli Machado D, Pegas Henriques JA. Differentiation of human adipose-derived adult stem cells into neuronal tissue: does it work? Differentiation 2009;77:221-228.
9. Banas A, Teratani T, Yamamoto Y, Tokuhara M, Takeshita F, Osaki M, et al. Rapid hepatic fate specification of adipose-derived stem cells and their therapeutic potential for liver failure. J Gastroenterol Hepatol 2009;24:70-77.
10. Banas A, Teratani T, Yamamoto Y, Tokuhara M, Takeshita F, Quinn G, et al. Adipose tissue-derived mesenchymal stem cells as a source of human hepatocytes. HEPATOLOGY 2007;46:219-228.
11. Uccelli A, Moretta L, Pistoia V. Immunoregulatory function of mesenchymal stem cells. Eur J Immunol 2006;36:2566-2573.
12. Zuk PA, Zhu M, Ashjian P, De Ugarte DA, Huang JI, Mizuno H, et al. Human adipose tissue is a source of multipotent stem cells. Mol Biol Cell 2002;13:4279-4295.
13. Matsuzawa N, Takamura T, Kurita S, Misu H, Ota T, Ando H, et al. Lipid-induced oxidative stress causes steatohepatitis in mice fed an atherogenic diet. HEPATOLOGY 2007;46:1392-1403.
14. Furuichi K, Shintani H, Sakai Y, Ochiya T, Matsushima K, Kaneko S, et al. Effects of adipose-derived mesenchymal cells on ischemia-reperfusion injury in kidney. Clin Exp Nephrol 2012;16:579-589.
15. Brunt EM. Nonalcoholic steatohepatitis: definition and pathology. Semin Liver Dis 2001;21:3-16.
16. Cohen JC, Horton JD, Hobbs HH. Human fatty liver disease: old questions and new insights. Science 2011;332:1519-1523.
17. Inzaugarat ME, Ferreyra Solari NE, Billordo LA, Abecasis R, Gadano AC, Chernavsky AC. Altered phenotype and functionality of circulating immune cells characterize adult patients with nonalcoholic steatohepatitis. J Clin Immunol 2011;31:1120-1130.
18. Alkhouri N, Morris-Stiff G, Campbell C, Lopez R, Tamimi TA, Yerian L, et al. Neutrophil to lymphocyte ratio: a new marker for predicting steatohepatitis and fibrosis in patients with nonalcoholic fatty liver disease. Liver Int 2012;32:297-302.
19. Susca M, Grassi A, Zauli D, Volta U, Lenzi M, Marchesini G, et al. Liver inflammatory cells, apoptosis, regeneration and stellate cell activation in non-alcoholic steatohepatitis. Dig Liver Dis 2001;33:768-777.
20. Olleros ML, Martin ML, Vesin D, Fotio AL, Santiago-Raber ML, Rubbia-Brandt L, et al. Fat diet and alcohol-induced steatohepatitis after LPS challenge in mice: role of bioactive TNF and Th1 type cytokines. Cytokine 2008;44:118-125.
21. Ferreyra Solari NE, Inzaugarat ME, Baz P, De Matteo E, Lezama C, Galoppo M, et al. The role of innate cells is coupled to a Th1-polarized immune response in pediatric nonalcoholic steatohepatitis. J Clin Immunol 2012;32:611-621.
22. Ouyang W, Kolls JK, Zheng Y. The biological functions of T helper 17 cell effector cytokines in inflammation. Immunity 2008;28:454-467.
23. Tang Y, Bian Z, Zhao L, Liu Y, Liang S, Wang Q, et al. Interleukin-17 exacerbates hepatic steatosis and inflammation in non-alcoholic fatty liver disease. Clin Exp Immunol 2011;166:281-290.
24. Wynn TA. Fibrotic disease and the T(H)1/T(H)2 paradigm. Nat Rev Immunol 2004;4:583-594.
25. Wu J, Zern MA. Hepatic stellate cells: a target for the treatment of liver fibrosis. J Gastroenterol 2000;35:665-672.
26. Wanninger J, Walter R, Bauer S, Eisinger K, Schaffler A, Dorn C, et al. MMP-9 activity is increased by adiponectin in primary human hepatocytes but even negatively correlates with serum adiponectin in a rodent model of non-alcoholic steatohepatitis. Exp Mol Pathol 2011;91:603-607.
27. Higashiyama R, Inagaki Y, Hong YY, Kushida M, Nakao S, Niioka M, et al. Bone marrow-derived cells express matrix metalloproteinases and contribute to regression of liver fibrosis in mice. HEPATOLOGY 2007;45:213-222.

Hepatology Research

Hepatology Research 2014; 44: E45–E53 doi: 10.1111/hepr.12208

Original Article

Characteristics and prediction of hepatitis B e-antigen negative hepatitis following seroconversion in patients with chronic hepatitis B

Susumu Morita,[1]* Akihiro Matsumoto,[1]* Takeji Umemura,[1] Soichiro Shibata,[1] Nozomi Kamijo,[1] Yuki Ichikawa,[1] Takefumi Kimura,[1] Satoru Joshita,[1] Michiharu Komatsu,[1] Kaname Yoshizawa[1,2] and Eiji Tanaka[1]

[1]*Department of Medicine, Shinshu University School of Medicine, Matsumoto, and* [2]*Department of Gastroenterology, National Hospital Organization Shinshu Ueda Medical Center, Ueda, Japan*

Aim: We analyzed the characteristics of alanine aminotransferase (ALT) abnormality after achieving hepatitis B e-antigen (HBeAg) seroconversion (SC) and other factors associated with the occurrence of HBeAg negative hepatitis.

Methods: We followed 36 patients with chronic hepatitis B from 3 years prior to at least 3 years after SC (mean, 11.6 years) and examined ALT, hepatitis B virus (HBV) DNA, HB surface antigen, HB core-related antigen (HBcrAg) levels and mutations related to HBeAg SC.

Results: ALT normalization (<31 IU/L for at least 1 year) was primarily observed until 2 years following SC, after which it became more infrequent. We next divided patients into abnormal (≥31 IU/L, $n = 20$) and normal (<31 IU/L, $n = 16$) groups based on integrated ALT level after the time point of 2 years from SC, and considered the former group as having HBeAg negative hepatitis in the present study. Although changes in median levels of ALT and HBcrAg differed significantly between the groups, multivariate analysis showed ALT normalization within 2 years after SC to be the only significant determining factor for this disease ($P = 0.001$). We then assessed the 19 patients whose ALT was normal at 2 years following SC, four of whom developed HBeAg negative hepatitis. Increased levels of HBV DNA ($P = 0.037$) and HBcrAg ($P = 0.033$) were significant factors of potential relevance.

Conclusion: ALT abnormality after 2 years of SC may be evaluated as HBeAg-negative hepatitis. ALT, HBV DNA and HBcrAg levels may be useful in predicting the outcome of patients who achieve HBeAg SC.

Key words: hepatitis B core-related antigen, hepatitis B virus, reactivation, seroconversion

INTRODUCTION

HEPATITIS B VIRUS (HBV) infection is a major health concern with an estimated 350–400 million carriers worldwide. Whereas acute infection in adults is generally self-limiting, that during early childhood develops into persistent infection in most individuals, which can lead to chronic hepatitis and eventually liver cirrhosis and hepatocellular carcinoma (HCC).[1–3] The natural history of chronic HBV infection can be classified into several phases based on levels of alanine aminotransferase (ALT) and HBV DNA, hepatitis B e-antigen (HBeAg) status and estimated immunological status.[4] In the immune tolerance phase, HBeAg is positive, ALT level is normal, histological evidence of hepatitis is absent or minimal, and HBV DNA level is elevated. The chronic hepatitis B phase is characterized by raised ALT and HBV DNA levels. In this phase, the host's immune system initiates a response that results in active hepatitis. In patients who are HBeAg positive, active hepatitis can be prolonged and may result in cirrhosis. However, chronic hepatitis B eventually transitions into an inactive phase with a loss of HBeAg positivity in the majority of patients. Seroconversion (SC) of HBeAg to HBe antibodies and the fall of HBV DNA level result in the disappearance of disease activity despite persisting hepatitis B surface antigen (HBsAg) and low HBV DNA level. The SC of

Correspondence: Dr Takeji Umemura, Department of Medicine, Shinshu University School of Medicine, 3-1-1 Asahi, Matsumoto 390-8621, Japan. Email: tumemura@shinshu-u.ac.jp
Conflict of interest: All authors declare no conflicts of interest.
*These authors contributed equally to this study.
Received 8 May 2013; revision 8 July 2013; accepted 10 July 2013.

HBeAg marks the transition from the hepatitis phase to the inactive carrier phase, which is generally thought to be a benign course for the HBV carrier, although hepatitis can sometimes reactivate spontaneously.[5]

Patients experiencing HBV reactivation undergo another transition characterized by increases in HBV DNA and ALT levels and disease activity without the reappearance of HBeAg. This phase is referred to as HBeAg negative chronic hepatitis B. Occasional severe hepatitis B flare-ups with moderate HBV DNA level occur in this phase.[6,7] It is thought that HBeAg negative chronic hepatitis B is caused by mutant strains of HBV that are unable to produce HBeAg[6,8] and tends to develop into cirrhosis and HCC more frequently than does HBeAg positive chronic hepatitis B.[9–13] Therefore, it is important to identify patients who are likely to develop HBeAg negative hepatitis after HBeAg SC from those who can maintain an inactive carrier phase. In the present study, we evaluated 36 patients with HBeAg SC to examine the effects of host factors and viral factors, including serum quantitative HBsAg, hepatitis B core-related antigen (HBcrAg), HBV DNA, PC (A1896) mutation and BCP mutations (T1762 and A1764) before, during and after SC.

METHODS

Patients

A TOTAL OF 36 patients with sustained HBeAg SC (24 men and 12 women; median age, 38 years [range, 23–65]) were enrolled in this study after meeting the following criteria: (i) follow ups for at least 3 years before and after HBeAg SC; and (ii) serum samples at several time points before, during and after SC available for testing. HBeAg SC was defined as seroclearance of HBeAg with the appearance of anti-HBe that was not followed by HBeAg reversion or loss of anti-HBe. All patients were seen at Shinshu University Hospital from 1985 to 2009. The median follow-up period after SC was 11.6 years (range, 3.2–26.0). HBsAg was confirmed to be positive on two or more occasions at least 6 months apart in all patients. No patients had other liver diseases, such as alcoholic or non-alcoholic fatty liver disease, autoimmune liver disease or drug-induced liver injury. Patients who were complicated with HCC or who showed signs of hepatic failure were excluded from the study. HBV genotype was C in all patients, who were also negative for antibodies to hepatitis C virus and HIV. Nucleoside/nucleotide analog (NUC) therapy was introduced in 14 patients after HBeAg SC on physicians' decision, and then follow up was stopped. No patient was treated with interferon during the study period. ALT, albumin, bilirubin, platelet and other relevant biochemical tests were performed using standard methods.[14] The integration value of ALT after SC was calculated using the method described by Kumada *et al.*[15] (median determination frequency, 4.7/year per person [range, 1.6–13.9]) because a previous study showed integration values to be more meaningful than arithmetic mean values in long-term follow-up cohorts.[16] As guidelines released by the Ministry of Health, Labor and Welfare of Japan advise consideration of antiviral therapy for patients with ALT levels of 31 IU/L or more,[17] an ALT integration value of less than 31 IU/L was defined as normal in this report. Serum samples were stored at −20°C until tested. Liver biopsies were performed by percutaneous sampling of the right lobe with a 14-G needle in eight patients with HBeAg negative hepatitis, as reported previously.[14] All biopsies were 1.5 cm or more in length. Liver histological findings were scored by the histology activity index of Knodell *et al.*[18] The protocol of this study was approved by the ethics committee of our university and was in accordance with the Declaration of Helsinki of 1975. Informed consent was obtained from each patient.

Hepatitis B viral markers

Serological markers for HBV, including HBsAg, HBeAg and anti-HBe, were tested using commercially available enzyme immunoassay kits (Abbott Japan, Tokyo, Japan).[19] Quantitative measurement of HBsAg was done using a chemiluminescence enzyme immunoassay (CLEIA)-based HISCL HBsAg assay manufactured by Sysmex (Kobe, Japan).[20] The assay had a quantitative range of −1.5 to 3.3 log IU/mL. Serum HBcrAg level was measured using a CLEIA HBcrAg assay kit with a fully automated Lumipulse System analyzer (Fujirebio, Tokyo, Japan) as described previously.[21] We expressed HBcrAg level in terms of log U/mL, with a quantitative range set at 3.0–6.8 log U/mL. End titers of HBsAg and HBcrAg were determined by diluting samples with normal human serum when initial results exceeded the upper limit of the assay range. HBV DNA level was measured using an Amplicor monitor assay with a dynamic range of 2.6–7.6 log copies/mL.[22] Six major genotypes (A–F) of HBV were determined using the method reported by Mizokami *et al.*,[23] in which the surface gene sequence amplified by polymerase chain reaction was analyzed by restriction fragment length polymorphism.

The PC and BCP mutations of HBV were assessed as previously described. Briefly, the stop codon mutation in the PC region (A1896) was detected with an enzyme-linked mini-sequence assay kit (Smitest; Roche Diagnostics, Tokyo, Japan) with a sensitivity of 1000 copies/mL. The results were expressed as the percent mutation rate as defined by Aritomi *et al.*[24] The PC mutation was judged to exist when the mutation rate exceeded 50% in the present study because the mutation rate would increase to 100% once surpassing this value.[25] The BCP double mutation was detected using an HBV core promoter detection kit (Smitest; Genome Science Laboratories) with a detection limit of 1000 copies/mL.[24] The BCP mutation was judged to exist for all classifications of mutant in the present study.

Statistical analysis

Clinical factors were compared between patients with and without HBeAg negative hepatitis after SC using the χ^2-test and Fisher's exact test, and group medians were compared using the Mann–Whitney *U*-test. Receiver-operator curves (ROC) with Youden's index were used to decide each cut-off point for predicting HBeAg negative hepatitis after SC. Differences between the analyzed groups were assessed using Kaplan–Meier analysis and the log-rank test. Sex, age at SC, HBcrAg level, ALT level, HBV DNA level, HBsAg level, PC mutation and BCP mutation were all suspected to be associated with ALT elevation after SC. Factors attaining a *P*-value of less than 20% in univariate analysis were used in multivariate analysis that employed a stepwise Cox proportional hazard model. These included level of serum albumin and platelet count at SC, levels of ALT at 0, 1, 2 and 3 years after SC, and levels of HBcrAg at 1, 2 and 3 years after SC. All tests were performed using the IBM SPSS Statistics Desktop for Japan ver. 19.0 (IBM Japan, Tokyo, Japan). *P*-values less than 0.05 were considered to be statistically significant.

RESULTS

Baseline characteristics of patients

ALL 36 PATIENTS enrolled showed abnormal levels of ALT before SC, with the majority showing normalization around the time of SC. We defined ALT normalization as a decrease in ALT level to less than 31 IU/L for at least 1 year. The change in ratio of patients not achieving normalization over time revealed two distinct phases (Fig. 1): the first was a fast decline phase from 2 years before SC to 2 years afterwards, and the second was a slow decline phase from 2 years after SC to the end of follow up. Normalization of ALT during the fast phase was presumed to be associated with HBeAg SC, which was seen in 53% (19/36) of total patients. Based on this, we analyzed the risk factors associated with ALT abnormality after the time point of 2 years from SC by calculating integrated ALT levels (Fig. 2). We defined patients whose integrated ALT level exceeded 30 IU/L as having HBeAg negative hepatitis in the present study. Serum HBV DNA of over 4.0 log copies/mL was observed in all patients with HBeAg negative hepatitis.

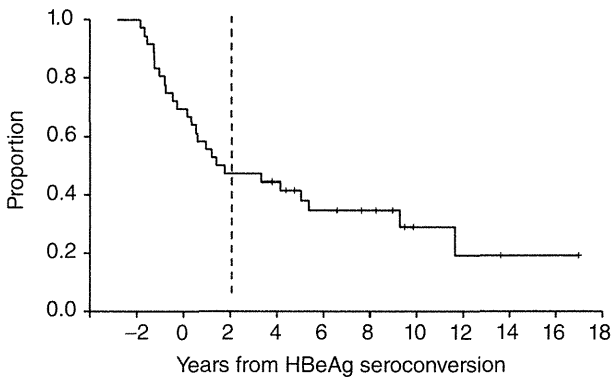

Figure 1 Changes in the proportion of patients with alanine aminotransferase (ALT) abnormality. ALT normalization was defined as ALT level decreasing to lower than 31 IU/L and maintained for at least 1 year. These data reveal two distinct time frames: a fast decline phase around the seroconversion (SC) period until 2 years afterwards, and a slow decline phase from 2 years after SC to the end of follow up. The vertical broken line at 2 years after SC indicates the borderline between the two phases. HBeAg, hepatitis B e-antigen.

Of the 36 patients enrolled, 20 (56%) developed HBeAg negative hepatitis and 16 (44%) did not. ALT normalization within 2 years after SC was significantly less frequent in patients with HBeAg negative hepatitis (Table 1). Median age, sex distribution and follow-up period did not differ between the two groups. Median albumin level tended to be lower in patients with HBeAg negative hepatitis, but only modestly. Eight of 20 HBeAg negative hepatitis patients underwent liver biopsy after SC. All had necroinflammatory activity. Initiation of NUC therapy was more common in the HBeAg negative hepatitis group.

Clinical and virological profiles

Changes in median levels of ALT, HBV DNA, HBsAg and HBcrAg during the course of SC have been compared between patients with and without HBeAg negative

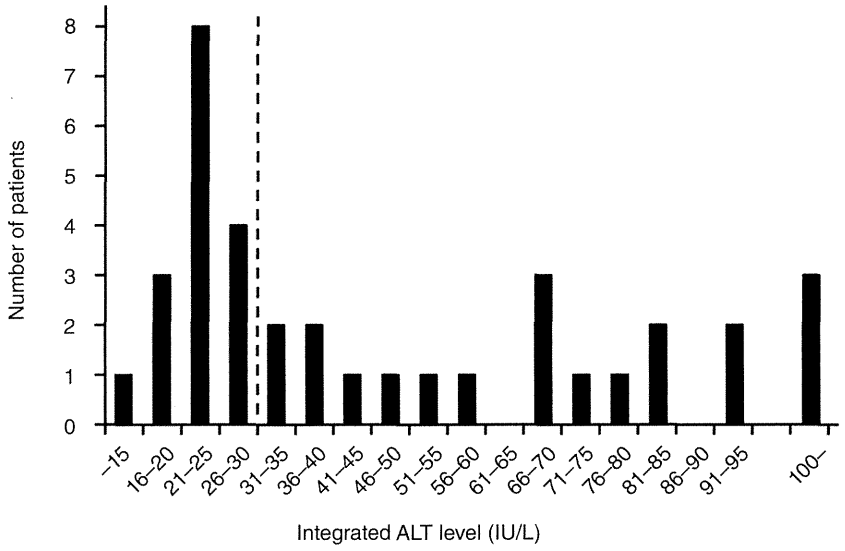

Figure 2 Distribution of integrated alanine aminotransferase (ALT) level from the time point of 2 years after seroconversion (SC) to the end of follow up.

hepatitis in Figure 3. We observed that median ALT level decreased around the time of SC in patients without HBeAg negative hepatitis, but did not in the other group. Overall, median ALT differed significantly between the two groups at the time of SC (43.0 vs 21.5 IU/L; $P = 0.009$) and at 1 (67.0 vs 15.0 IU/L; $P = 0.001$), 2 (52.0 vs 14.5 IU/L; $P < 0.001$) and 3 years (41.5 vs 15.0 IU/L; $P < 0.001$) afterwards (Fig. 3a). Median HBV DNA level decreased similarly in both groups around the time of SC (Fig. 3b). Median HBsAg level was unchanged or minimally decreased in both groups around the time of SC, but was significantly lower in patients with HBeAg negative hepatitis at 1 (3.9 vs 3.2 log IU/mL; $P = 0.025$) and 2 years (3.9 vs 3.2 log IU/mL; $P = 0.045$) before SC and at 2 years (3.7 vs 3.0 log IU/mL; $P = 0.023$) after SC (Fig. 3c). Median HBcrAg level decreased in both groups around the time of SC, but this decline was more gradual in patients with HBeAg negative hepatitis, becoming significantly higher at 1 (5.2 vs 3.9 log U/mL; $P = 0.011$), 2 (4.6 vs 3.5 log

Table 1 Comparison of host and viral factors between patients with and without HBeAg negative hepatitis among total patients

Clinical characteristics	HBeAg negative hepatitis		*P*
	Present ($n = 20$)	Absent ($n = 16$)	
Age at SC (years)†	40 (23–64)	38 (24–65)	0.504
Sex (male : female)	15:5	9:7	0.298
Follow-up period (years)†	10.6 (3.8–26.0)	12.4 (3.2–23.1)	0.610
Laboratory data at SC			
Albumin (g/dL)†	4.1 (3.6–4.6)	4.3 (3.7–4.8)	0.030
Bilirubin (mg/dL)†	1.0 (0.4–2.6)	0.8 (0.5–1.3)	0.319
Platelets (/μL)†	13.9 (8.5–24.3)	18.1 (9.6–22.9)	0.187
ALT normalization within 2 years after SC‡	4 (20)	15 (94)	<0.001
Events during follow-up period			
Initiation of NUC therapy‡	12 (60)	2 (13)	0.006
Development of HCC‡	2 (10)	1 (6)	1.000

†Data are expressed as median (range).
‡Data are expressed as number of patients (%).
ALT, alanine aminotransferase; HBeAg, hepatitis B e-antigen; HCC, hepatocellular carcinoma; NUC, nucleoside/nucleotide analog; SC, seroconversion.

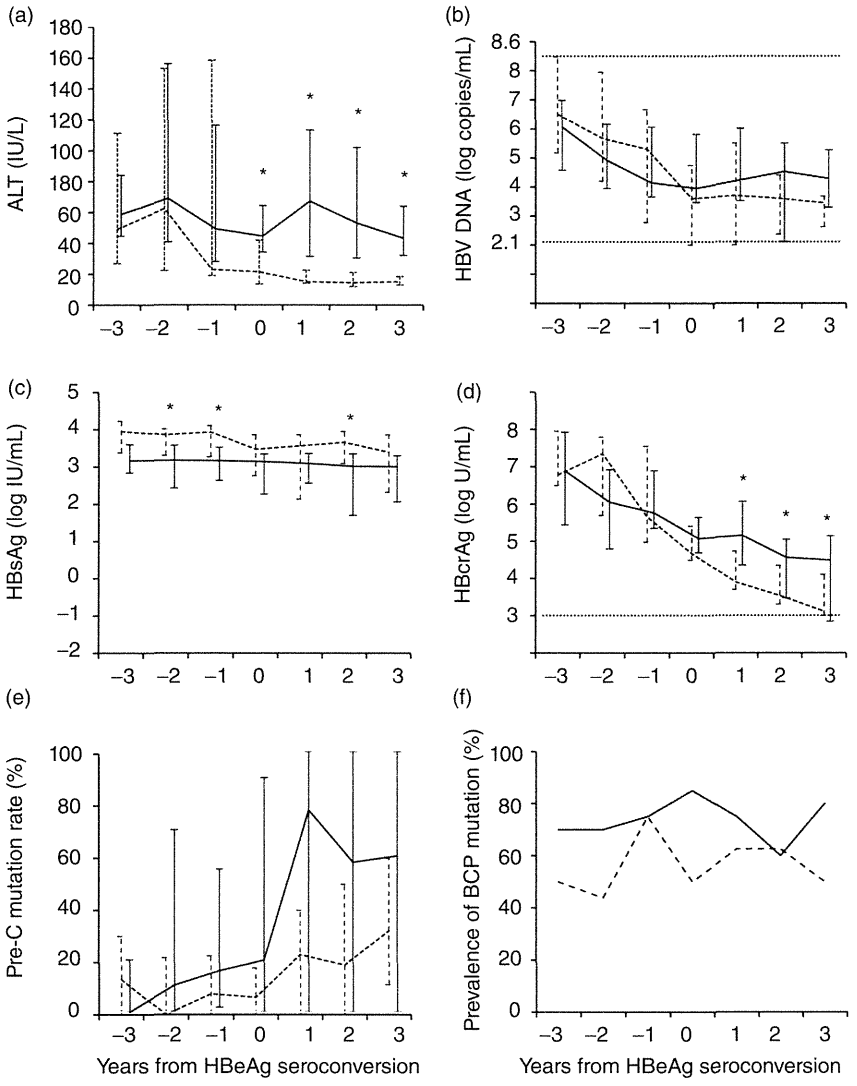

Figure 3 Changes in median levels of serum alanine aminotransferase (ALT) (a), hepatitis B virus (HBV) DNA (b), hepatitis B surface antigen (HBsAg) (c), hepatitis B core-related antigen (HBcrAg) (d) and PC mutation rate (e) are compared between patients with and without the occurrence of hepatitis B e-antigen (HBeAg) negative hepatitis. A similar comparison is made for prevalence of patients with BCP mutations (f). Solid lines indicate patients with HBeAg negative hepatitis ($n = 20$) and broken lines indicate those without ($n = 16$). Data are shown as median values with 25% and 75% ranges at each point for (a–e). Horizontal broken lines in (b) and (d) indicate the upper and lower detection limits of the corresponding markers. $^*P < 0.05$.

U/mL; $P = 0.041$) and 3 years (4.6 vs 3.1 log U/mL; $P = 0.016$) after SC (Fig. 3d). PC mutation rate increased similarly in both groups during the course of SC (Fig. 3e), and the prevalence of BCP mutation positive patients remained comparatively high in both groups throughout the study period (Fig. 3f).

All factors that were associated with the occurrence of HBeAg negative hepatitis were evaluated for independence by multivariate analysis. We found that only abnormal level of ALT (≥31 IU/L) at 2 years after SC (odds ratio, 42.0; 95% confidence interval, 4.3–405.4; $P = 0.001$) was an independent predictive factor. Therefore, we examined for factors associated with the occurrence of HBeAg negative hepatitis in the 19 patients whose ALT level had normalized by 2 years after SC. Four (21%) of these patients developed HBeAg negative hepatitis and the remaining 15 (79%) did not. We found no significant differences between the two groups with regard to age at SC, sex or laboratory data (Table 2). We next analyzed HBV DNA, HBsAg and HBcrAg levels at 2 years after SC to see if these factors could discriminate between patients with and without the development of HBeAg negative hepatitis. Cut-off values for each factor were determined by ROC analysis. As shown in Figure 4, serum levels of HBV DNA (7% vs 60%; $P = 0.037$) and HBcrAg (0% vs 44%; $P = 0.033$) were significant factors indicating susceptibility, but HBsAg was not.